NACA

RESEARCH MEMORANDUM

THE EFFECT OF GROUND ON THE LOW-SPEED AERODYNAMIC, CONTROL, AND CONTROL HINGE-MOMENT CHARACTERISTICS OF A DELTA-WING—FUSELAGE MODEL WITH TRAILING-EDGE CONTROLS

By William I. Scallion

Langley Aeronautical Laboratory
Langley Field, Va.

NATIONAL ADVISORY COMMITTEE
FOR AERONAUTICS

WASHINGTON

September 24, 1954

NACA RM L54H03 [redacted]

NATIONAL ADVISORY COMMITTEE FOR AERONAUTICS

RESEARCH MEMORANDUM

THE EFFECT OF GROUND ON THE LOW-SPEED AERODYNAMIC, CONTROL, AND CONTROL HINGE-MOMENT CHARACTERISTICS OF A DELTA-WING—FUSELAGE MODEL WITH TRAILING-EDGE CONTROLS

By William I. Scallion

SUMMARY

An investigation was made in the Langley full-scale tunnel to determine the effect of ground on the low-speed aerodynamic, control, and control hinge-moment characteristics of a 3-percent-thick, delta-wing—fuselage configuration. The model had inboard trailing-edge flaps and outboard horn-balance-type ailerons of 10.8 and 10.2 percent total wing area, respectively. Aerodynamic forces and moments and hinge-moment data were obtained for an angle-of-attack range of -3.7° to 36.3° at several ground heights at a test Reynolds number of 2.3×10^6 and a Mach number of 0.10.

The effects of ground on the longitudinal characteristics of the delta wing were small and were similar to those of swept and unswept wings in the same range of ground heights. The longitudinal- and lateral-control effectiveness was not greatly affected by the presence of the ground at the ground heights tested. A decrease in ground height extended the lift-coefficient range in which the flap deflection required for zero pitching moment was greater than the flap deflection for zero hinge moment in the range of ground heights tested.

INTRODUCTION

Flights of experimental delta-wing airplanes have indicated that the presence of the ground might seriously affect the low-speed handling qualities during the landing maneuver. Inasmuch as previous ground-effect studies of swept- and delta-wing configurations (refs. 1 and 2) were not concerned directly with the effect on control, opportunity was taken to make such a study of an available 60° delta-wing—fuselage configuration

equipped with trailing-edge controls. The configuration, which had already been studied in some detail (ref. 3), had a 3-percent-thick wing equipped with inboard trailing-edge flaps and outboard horn-balance-type ailerons.

The tests were made in the presence of a ground board in the Langley full-scale tunnel. They included the longitudinal characteristics of the model and the control and control hinge-moment characteristics of trailing-edge flaps and horn-balance-type ailerons with areas of 10.8 and 10.2 percent total wing area, respectively. Forces and moments as well as control hinge moments were obtained in the angle-of-attack range from -3.7° through the angle for maximum lift at several ground heights. The test Reynolds number was 2.3×10^6 and the Mach number was 0.10.

COEFFICIENTS AND SYMBOLS

All results are presented in standard NACA form of coefficients of forces and moments. Wing forces and moments are referred to the stability axes originating at the projection of the quarter-chord point of the mean aerodynamic chord on the plane of symmetry. The positive directions of forces, moments, and angles are shown in figure 1.

C_L lift coefficient, $\frac{\text{Lift}}{qS}$

C_D drag coefficient, $\frac{\text{Drag}}{qS}$

C_m pitching-moment coefficient, $\frac{\text{Pitching moment}}{qS\bar{c}}$

C_n yawing-moment coefficient, $\frac{\text{Yawing moment}}{qSb}$

C_l rolling-moment coefficient, $\frac{\text{Rolling moment}}{qSb}$

C_h hinge-moment coefficient, $\frac{\text{Hinge moment}}{2qQ}$

$C_{L_{max}}$ maximum lift coefficient

u local velocity on surface, ft/sec

H hinge moment, ft-lb

ρ	mass density of air, slugs/cu ft
V	free-stream velocity, ft/sec
q	free-stream dynamic pressure, lb/sq ft
S	total wing area (based on theoretical tip), sq ft
Q	moment of area of control surface rearward of hinge line about hinge line, ft^3
$\bar{c}$	wing mean aerodynamic chord measured parallel to plane of symmetry, $\frac{2}{S}\int_0^{b/2} c^2 dy$, ft
c	wing chord measured parallel to plane of symmetry, ft
b	wing span, ft
x	distance along longitudinal axis, ft
y	distance along lateral axis, ft
α	angle of attack of wing chord line, deg
δ	control deflection, deg
h	height of $0.25\bar{c}$ point on wing above ground plane, ft
C_{m_δ}	rate of change of pitching-moment coefficient with control deflection (slope at zero deflection), per deg
C_{n_δ}	rate of change of yawing-moment coefficient with control deflection (slope at zero deflection), per deg
C_{l_δ}	rate of change of rolling-moment coefficient with control deflection (slope at zero deflection), per deg
C_{h_δ}	rate of change of hinge-moment coefficient with control deflection (slope at zero deflection), per deg

Subscripts:

a	horn-balance-type aileron on right semispan
f	flaps on both semispans

i inboard flap segment

o outboard flap segment

MODEL AND GROUND BOARD

Model

The model in this investigation had a delta-plan-form wing with the leading edge swept back 60°, an aspect ratio of 2.31, and NACA 65A003 airfoil sections parallel to the model axis of symmetry. The wing root chord was located on the fuselage center line. Coordinates for the fuselage and wing are given in tables I and II. The controls were of the trailing-edge type, the hinge line being located at 0.88 wing root chord, and were divided into three segments. The two inboard segments on each semispan were deflected as a flap during the tests and were 10.8 percent of the total wing area. The outboard segments were horn-balance-type ailerons that were 10.2 percent of the total wing area. The balance area ahead of the hinge line was 14 percent of the total aileron area. The general arrangement of the model and controls is given in figure 2.

Ground Board

The ground board used in this investigation is shown in figures 3 and 4 and consisted of a wood framework covered with plywood on the upper and lower surfaces with an overall thickness of $2\frac{2}{8}$ inches and with a rounded leading edge and a blunt trailing edge. The board was 16 feet long and 14 feet wide and was supported on pipe columns which had adjustable lengths. A diagram of the relative positions of the model and the ground board is shown in figure 3.

METHODS AND TESTS

The model was sting mounted, the angle-of-attack pivot point being located on the model center line 5.76 feet behind the model center of gravity on the wing. This arrangement was not entirely satisfactory because the height of the model center of gravity above the ground board varied with angle of attack. In order to provide a range of ground heights at specific angles of attack, it was necessary to vary the ground-board height for each sequence of tests (see fig. 3).

The model was tested at an angle-of-attack range of -3.7° to 36.3° with the ground board located 2.58 and 1.58 feet below the angle-of-attack

pivot point. Some tests were made with the ground board located 0.42 foot above the angle-of-attack pivot point; however, the angles of attack for these tests were limited to the higher range (between 24.3° and 36.3°).

The characteristics of the model controls were obtained at all ground heights tested. The flap segments were deflected as a unit on both semispans for deflection angles of -10°, 0°, and 20°. The aileron was deflected -10°, 0°, and 10° on the right semispan only. Aerodynamic forces, moments, and hinge moments were obtained by use of a six-component strain-gage balance in the fuselage and strain-gage beams attached to the control surfaces. The test Reynolds number was 2.3×10^6 based on the wing mean aerodynamic chord, and the Mach number was 0.10.

The data have been corrected for an average stream angle of 0.3° based on surveys with the ground board installed. Calculations were made to determine the jet-boundary correction with the ground board out (by the method of ref. 4) and the buoyancy correction, but these corrections were found to be negligible and therefore were not applied.

Prior to actual testing, the boundary-layer conditions on the ground board were observed. Boundary-layer measurements on the ground board under the model and $1.16\bar{c}$ behind the model center of gravity indicated that the maximum thickness of the boundary layer (absolute height to $u/V = 1.0$) beneath the model was approximately 1 inch thick and was approximately 2 inches thick $1.16\bar{c}$ behind the model center of gravity. Visual tuft studies of the flow on the ground-board surface were made through the angle-of-attack range of the model, and no indication of separation was observed.

PRESENTATION OF DATA

The basic data are not presented in their entirety. Figures 5(a) to 5(e), however, are typical examples of the form in which the data are obtained for this investigation. In these figures, C_L, C_m, C_D, C_y, C_n, C_l, and C_h are plotted against h/b, the height-span ratio. Data at a constant h/b value were obtained by cross-plotting the basic data. All subsequent figures are plotted in this manner for h/b values of 1.0, 0.7, and 0.4. Symbols are used in these figures merely to identify and distinguish the curves and do not indicate actual test points. The portions of the curves that are dashed lines were cross-plotted from extrapolated-data curves similar to those in figure 5.

In figure 6, the longitudinal characteristics are presented with the flaps deflected 0°, -10°, and 20°. Figure 7 shows the effect of ground height on maximum lift coefficient at these three flap deflections. The variation of hinge-moment coefficient with angle of attack at several

ground heights for the horn-balance-type aileron is given in figure 8, for each segment of the flaps with both segments deflected together as a unit in figures 9(a) and 9(b), and for the complete flap in figure 9(c). The variation of pitching-moment coefficient, yawing-moment coefficient, rolling-moment coefficient, and hinge-moment coefficient with horn-balance-type aileron deflection is presented in figures 10 to 13, respectively.

The longitudinal-control and hinge-moment characteristics of the flaps are shown in figures 14 and 15 as the variation of C_m and C_h against δ_f. The control and hinge-moment parameters, C_{n_δ}, C_{l_δ}, C_{m_δ} and C_{h_δ} of the horn-balance-type aileron, and C_{m_δ} and C_{h_δ} of the flaps, are plotted against lift coefficient in figures 16 to 20.

Figure 21 shows the effect of decreasing ground height on the control deflection required for trim (δ_f at $C_m = 0$) and the control floating angle (δ_f at $C_h = 0$) of the flaps in the complete lift-coefficient range. The δ_f values at the high lift coefficients were obtained by extrapolating the curves of figures 14 and 15 and are considered approximate.

RESULTS AND DISCUSSION

Longitudinal Characteristics

The slope of the lift curve below $C_L = 0.6$ increased with a decrease in ground height between $h/b = 0.7$ and $h/b = 0.4$ when the controls were neutral (fig 6(a)) or the flaps were deflected -10° (fig. 6(b)). When the flaps were deflected 20°, the lift-curve slope at lift coefficients below $C_L = 0.6$ was relatively unchanged by decreasing ground height to $h/b = 0.4$ (fig. 6(c)). These characteristics are generally similar to those reported for the swept and delta wings of references 1 and 2, respectively.

The data of figure 7 show an increase in maximum lift coefficient between $h/b = 0.8$ and $h/b = 0.4$ for the model with flaps neutral; however, the actual increment is small (0.07). The values of maximum lift coefficient at $h/b = \infty$ for this configuration are not available; however, at $h/b = 1.0$, they are comparable to those of similar delta-wing configurations at $h/b = \infty$ (refs. 5 and 6) in which the maximum lift coefficients with controls neutral are approximately 1.2. There is a small increase in maximum lift coefficient with a decrease in ground height with the flaps deflected -10°. There is essentially no change in the maximum lift coefficient with a decrease in ground height when the flaps are deflected 20°. A reduction in maximum lift coefficient at small ground heights might have been expected on the basis of the results

of reference 1; however, this wing utilized flaps through greater deflections than the delta-wing model of this investigation and, therefore, was effectively more highly cambered. As mentioned in reference 1, the negative induced angle and camber effects are possibly more pronounced on highly cambered wings.

Decreasing ground height caused slight reductions in drag between $h/b = 0.7$ and $h/b = 0.4$ at flap deflections of 0° and 20° (fig. 6(d)).

Proximity to the ground had only a small effect on the longitudinal stability of the model (figs. 6(a), 6(b), and 6(c)). A slight increase in longitudinal stability at high lift coefficients occurred at the lowest ground height, $h/b = 0.4$, when the flaps were neutral or deflected -10°.

CONTROL CHARACTERISTICS

Longitudinal

The longitudinal control effectiveness of the flaps (fig. 20) remained fairly constant ($C_{m_\delta} = -0.0054$) throughout most of the lift-coefficient range at $h/b = 1.0$ and was not appreciably changed when h/b was reduced to 0.4.

Lateral

The yawing-moment characteristics with the horn-balance-type aileron deflected (figs. 16 to 18) were adverse ($+C_{n_\delta}$) throughout the lift-coefficient range and were not materially affected by changes in height above the ground.

The effects of a decrease in ground height on the lateral-control effectiveness C_{l_δ} of the horn-balance-type control were generally small and, because the changes that were noted did not follow any particular pattern, no definite variation of $C_{l_{\delta_a}}$ with ground height can be established (figs. 16 to 18). There was a reduction in $C_{l_{\delta_a}}$ at high lift coefficients at all ground heights tested, the most notable case being that in which the flaps were deflected 20° (fig. 18). A similar reduction in $C_{l_{\delta_a}}$ due to deflection of flaps is shown for an identical but large-scale configuration in reference 7.

Hinge-Moment Characteristics

Proximity to ground had little effect on the hinge-moment characteristics of the aileron when the flaps were neutral or deflected -10°;

however, a slight reduction in $C_{h_{\delta_a}}$ with decreasing ground height occurred above $C_L \approx 0.8$ when the flaps were deflected 20° (fig. 19).

As shown in figure 9, the effect of reducing ground height on the flap segments and the flap as a whole was to increase slightly the slope of the curve of C_h against α above $\alpha = 16.3°$ at flap deflections of 0° and -10°. The flap hinge-moment parameter $C_{h_{\delta_f}}$ was reduced slightly above $C_L = 0.5$ when h/b was decreased from 1.0 to 0.4 (fig. 20).

The combined effects of proximity to ground on the control-effectiveness and hinge-moment characteristics of the flaps are summarized in figure 21, in which the flap deflection required for trim and the flap floating angle are given throughout the lift-coefficient range for ground heights of $h/b = 1.0$ and $h/b = 0.4$. The absolute values of flap deflection required for trim used in this figure are based on a center-of-gravity position at $0.25\bar{c}$ and should not be construed to be applicable to any other center-of-gravity location. At $h/b = 1.0$, the flap floating angle exceeded the flap deflection required for trim at high lift coefficients. This condition is unsatisfactory for the model with the chosen center-of-gravity location; however, as the ground height was decreased to $h/b = 0.4$, the point at which the curves coincided was extended to maximum lift.

SUMMARY OF RESULTS

The results of the low-speed investigation of the aerodynamic, control, and control hinge-moment characteristics near the ground of a 3-percent-thick, 60° sweptback delta-wing—fuselage combination with inboard trailing-edge and horn-balance-type controls of 10.8- and 10.2-percent total wing area, respectively, may be summarized as follows:

1. The effects of proximity to ground on the longitudinal characteristics of the delta-wing model (lift, drag, and longitudinal stability) were similar in nature to those of swept and unswept wings, within the same range of ground heights tested. There was, in general, an increase in lift-curve slope, a slight increase in maximum lift coefficient with the controls neutral, a decrease in drag coefficient, and only minor changes in longitudinal stability at small ground heights.

2. The longitudinal control effectiveness of the flaps and the lateral control effectiveness of the horn-balance-type ailerons were not greatly affected by the presence of the ground for the ground heights tested.

3. Proximity to the ground had only small effect on the hinge-moment characteristics of the horn-balance-type aileron and flap.

4. A decrease in ground height extended the lift-coefficient range in which the flap deflection required for zero pitching moment was greater than the floating angle of the flap (the flap deflection for zero hinge moment) in the range of ground heights tested.

Langley Aeronautical Laboratory,
National Advisory Committee for Aeronautics,
Langley Field, Va., July 15, 1954.

REFERENCES

1. Furlong, G. Chester, and Bollech, Thomas V.: Effect of Ground Interference on the Aerodynamic Characteristics of a 42° Sweptback Wing. NACA TN 2487, 1951.

2. Reibe, John M., and Graven, Jean C., Jr.: Low-Speed Investigation of the Effects of Location of a Delta Horizontal Tail on the Longitudinal Stability and Control of a Fuselage and Thin Delta Wing With Double Slotted Flaps Including the Effects of a Ground Board. NACA RM L53H19a, 1953.

3. Scallion, William I.: Low-Speed Investigation of the Aerodynamic, Control, and Hinge-Moment Characteristics in Sideslip of a Delta-Wing—Fuselage Model With Horn-Balance-Type Ailerons and With and Without Nacelles. NACA RM L53G09b, 1953.

4. Katzoff, S., and Hannah, Margery E.: Calculation of Tunnel-Induced Upwash Velocities for Swept and Yawed Wings. NACA TN 1748, 1948.

5. Wolhart, Walter D., and Michael, William H., Jr.: Wind-Tunnel Investigation of the Low-Speed Longitudinal and Lateral Control Characteristics of a Triangular-Wing Model of Aspect Ratio 2.31 Having Constant-Chord Control Surfaces. NACA RM L50G17, 1950.

6. Gottlieb, Stanley M.: Low-Speed Investigation of the Lateral Control Characteristics of a Series of Three Tip Ailerons on a 60° Triangular Wing. NACA RM L53F16a, 1953.

7. Fink, Marvin P., and Cocke, Bennie W.: A Low-Speed Investigation of the Aerodynamic, Control, and Hinge-Moment Characteristics of Two Types of Controls and Balancing Tabs on a Large-Scale Thin Delta-Wing—Fuselage Model. NACA RM L54B03, 1954.

TABLE I

FUSELAGE ORDINATES

x, in.	y, in.
0	0
.72	.333
1.08	.4284
1.80	.6156
3.60	1.040
7.20	1.735
10.80	2.322
14.40	2.838
21.60	3.733
28.80	4.449
36.00	4.989
43.20	5.387
50.40	5.662
57.60	5.850
64.80	5.965
72.00	6.001
79.20	5.947
86.40	5.794
93.60	5.466
100.80	5.128
108.00	4.789
115.20	4.453
120.00	4.224

TABLE II

NACA 65A003 AIRFOIL ORDINATES

Station, percent chord	y, percent chord
0	0
.5	.234
.75	.284
1.25	.362
2.50	.493
5.00	.658
7.50	.796
10.00	.912
15.00	1.097
20.00	1.236
25.00	1.342
30.00	1.420
35.00	1.472
40.00	1.498
45.00	1.497
50.00	1.465
55.00	1.402
60.00	1.309
65.00	1.191
70.00	1.053
75.00	.897
80.00	.727
85.00	.549
90.00	.369
95.00	.188
100.00	.007
Leading-edge radius, 0.057 percent c	

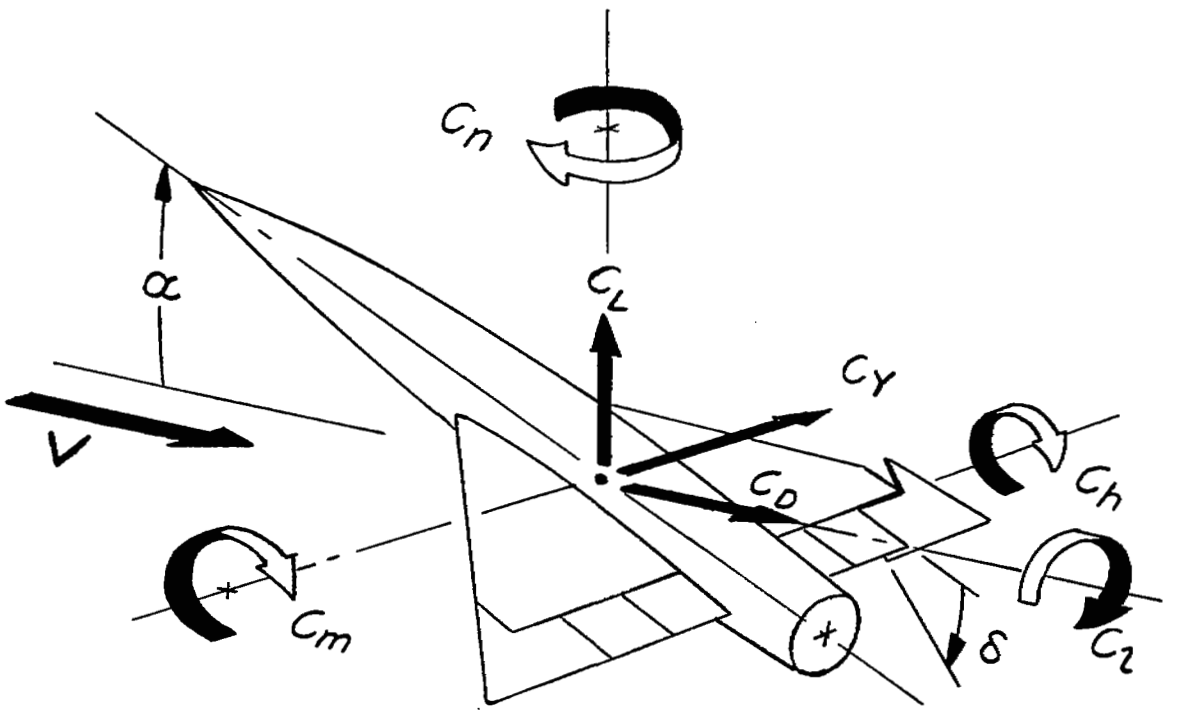

Figure 1.- System of axes used. Arrows indicate positive direction of forces, moments, and angular displacements.

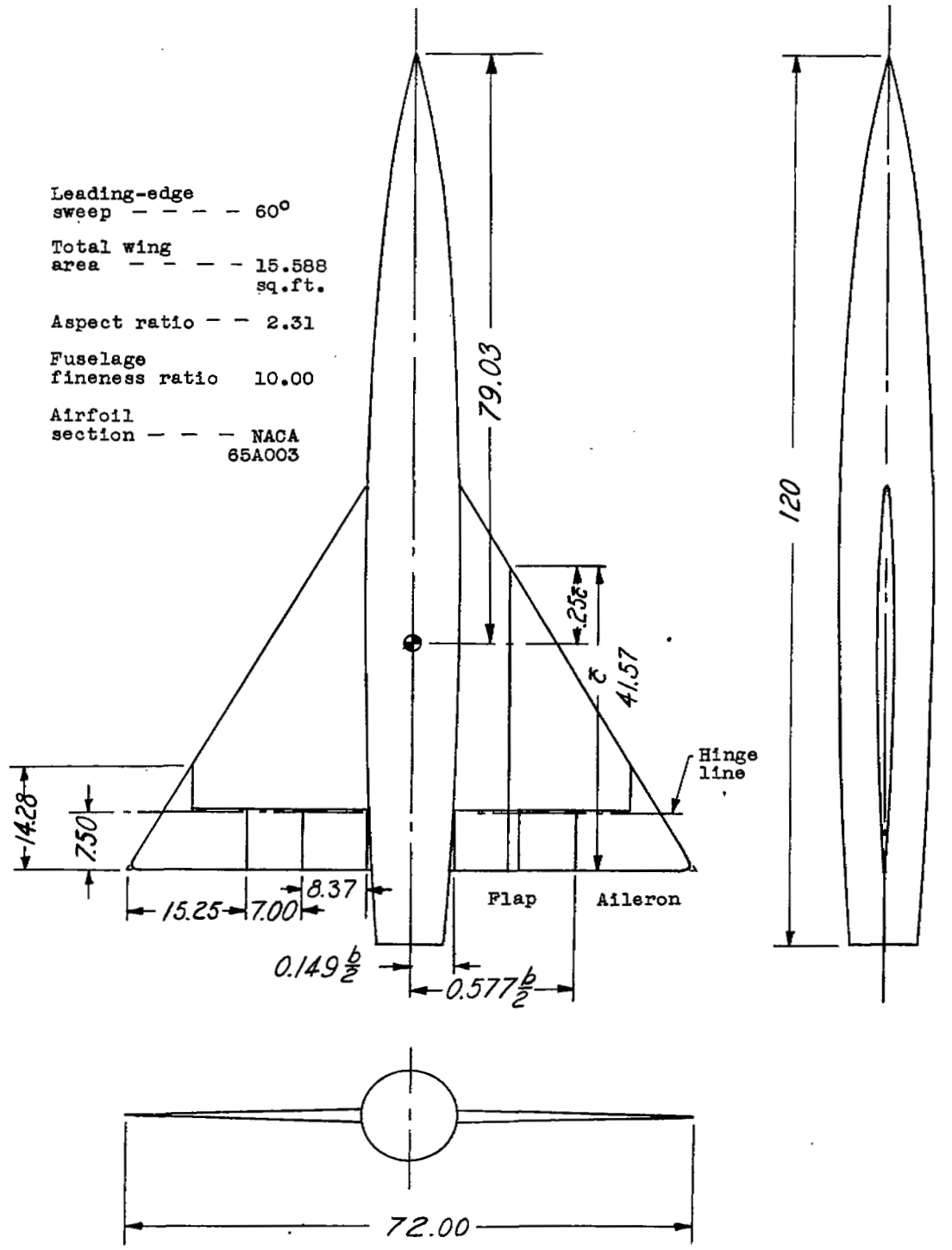

Figure 2.- General arrangement and principal dimensions of the 60° delta-wing model. All dimensions are given in inches.

[redacted]

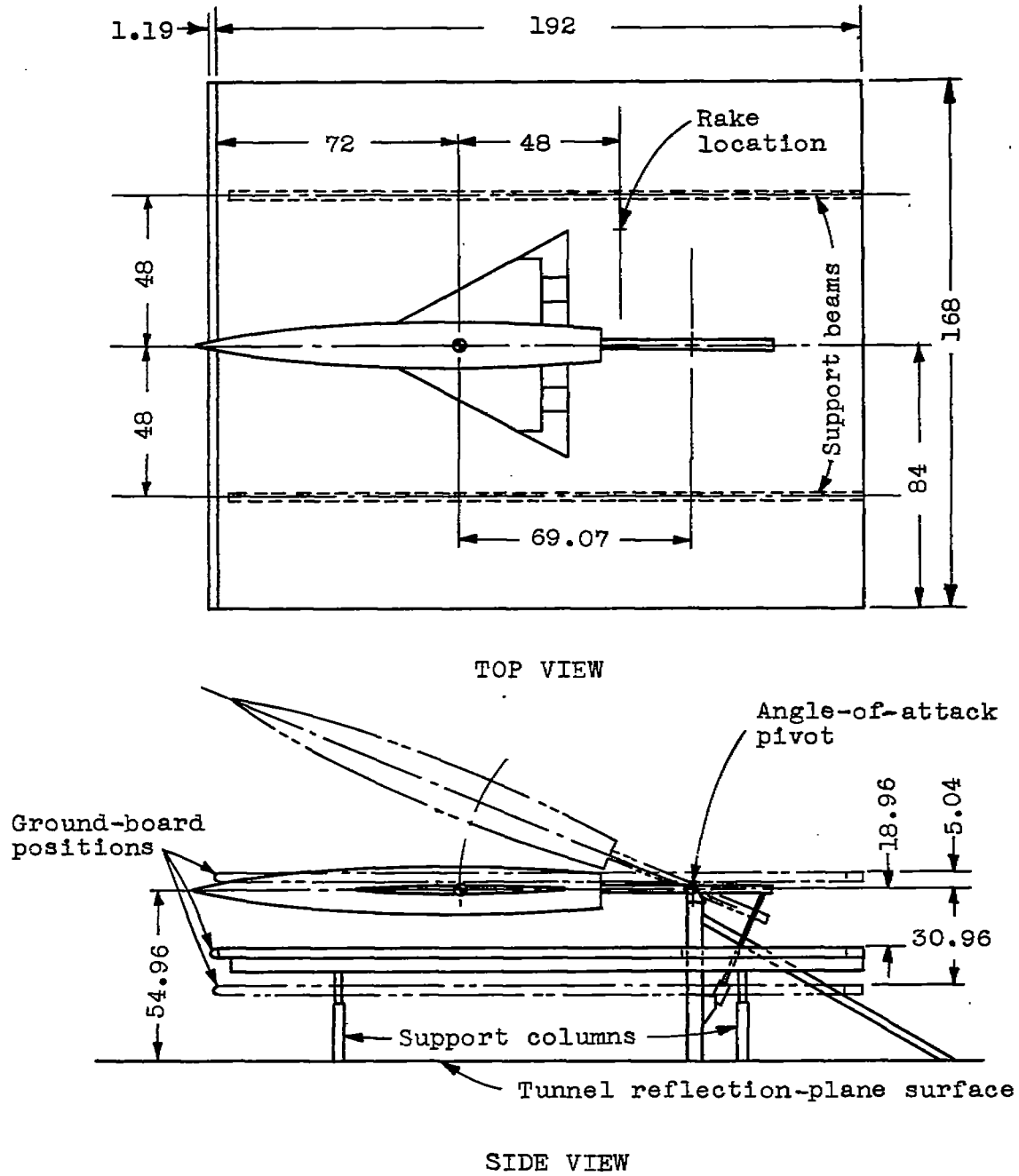

Figure 3.- Details and dimensions of the ground board showing its positions relative to the delta-wing model. All dimensions are given in inches.

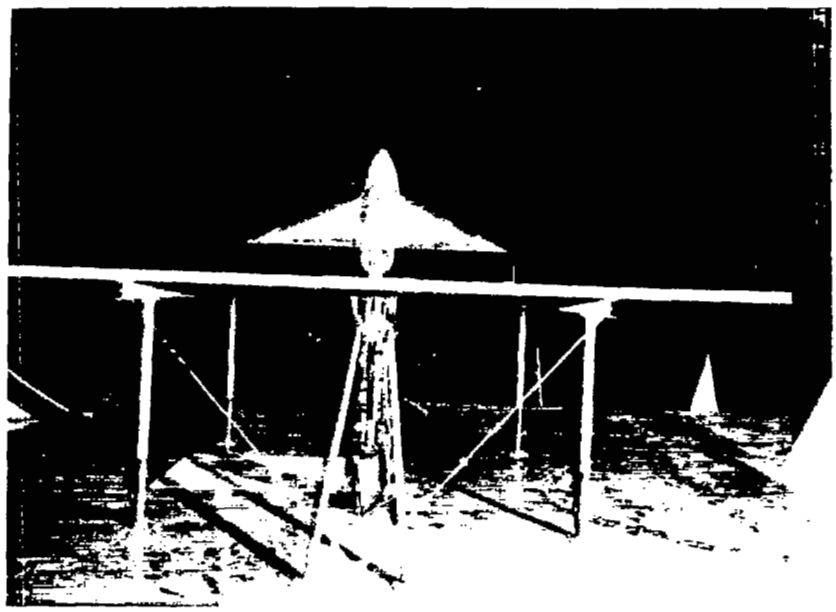

L-79706

(a) Rear view.

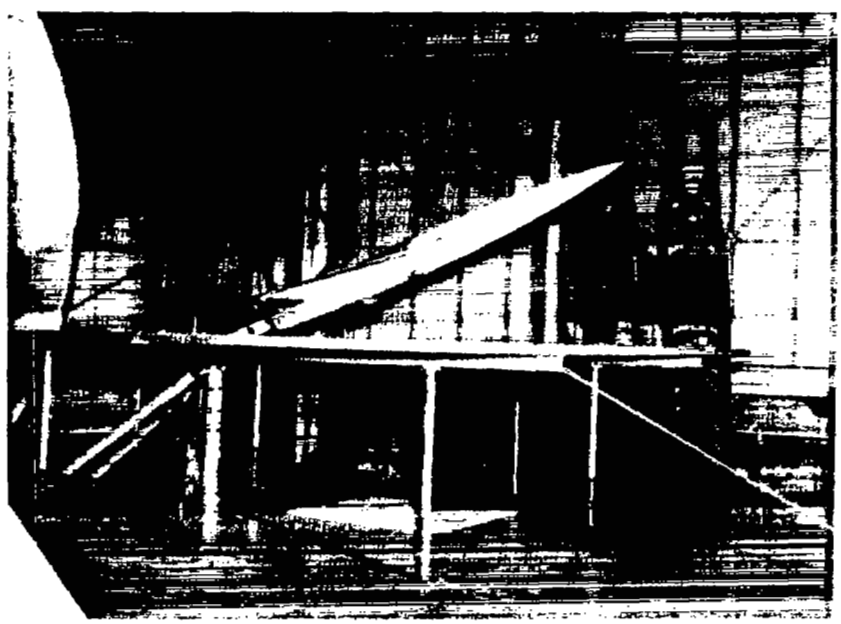

L-79705

(b) Side view.

Figure 4.- Photographs of the delta-wing model and ground board mounted in the Langley full-scale tunnel.

[redacted]

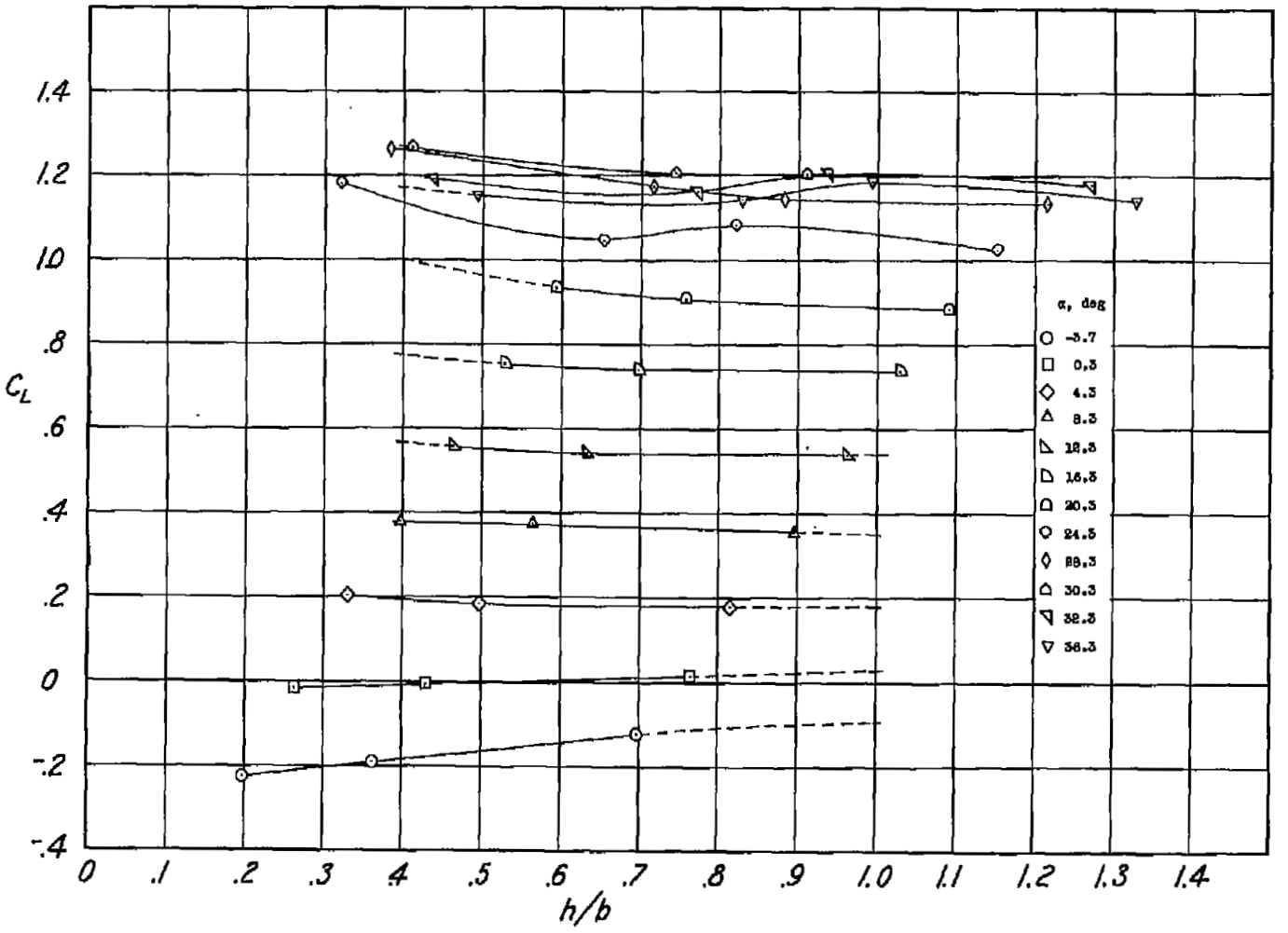

(a) Lift coefficient.

Figure 5.- Variation of the aerodynamic characteristics of the delta-wing model with height span ratio at several angles of attack. $\delta_f = 0^\circ$; $\delta_a = 0^\circ$.

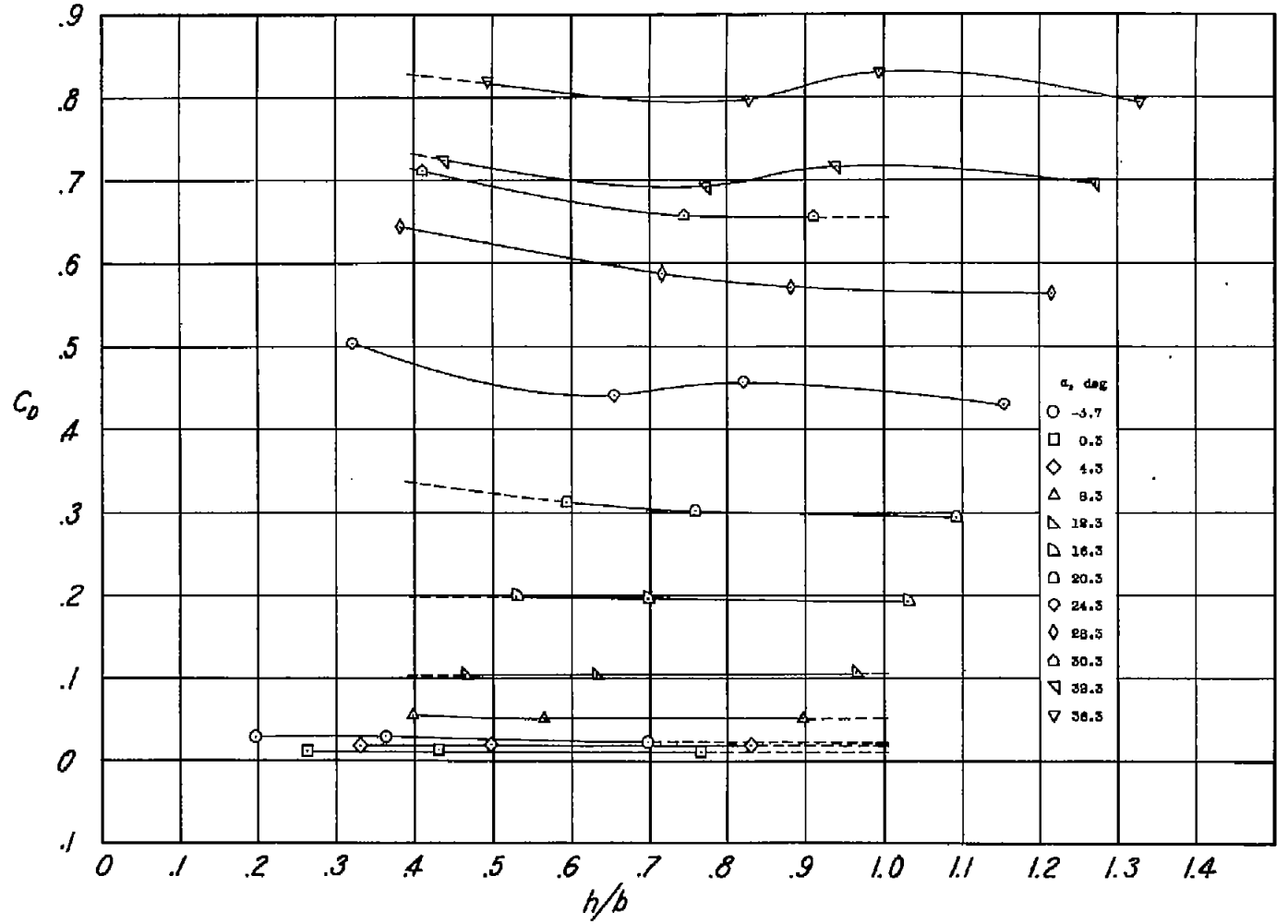

(b) Drag coefficient.

Figure 5.- Continued.

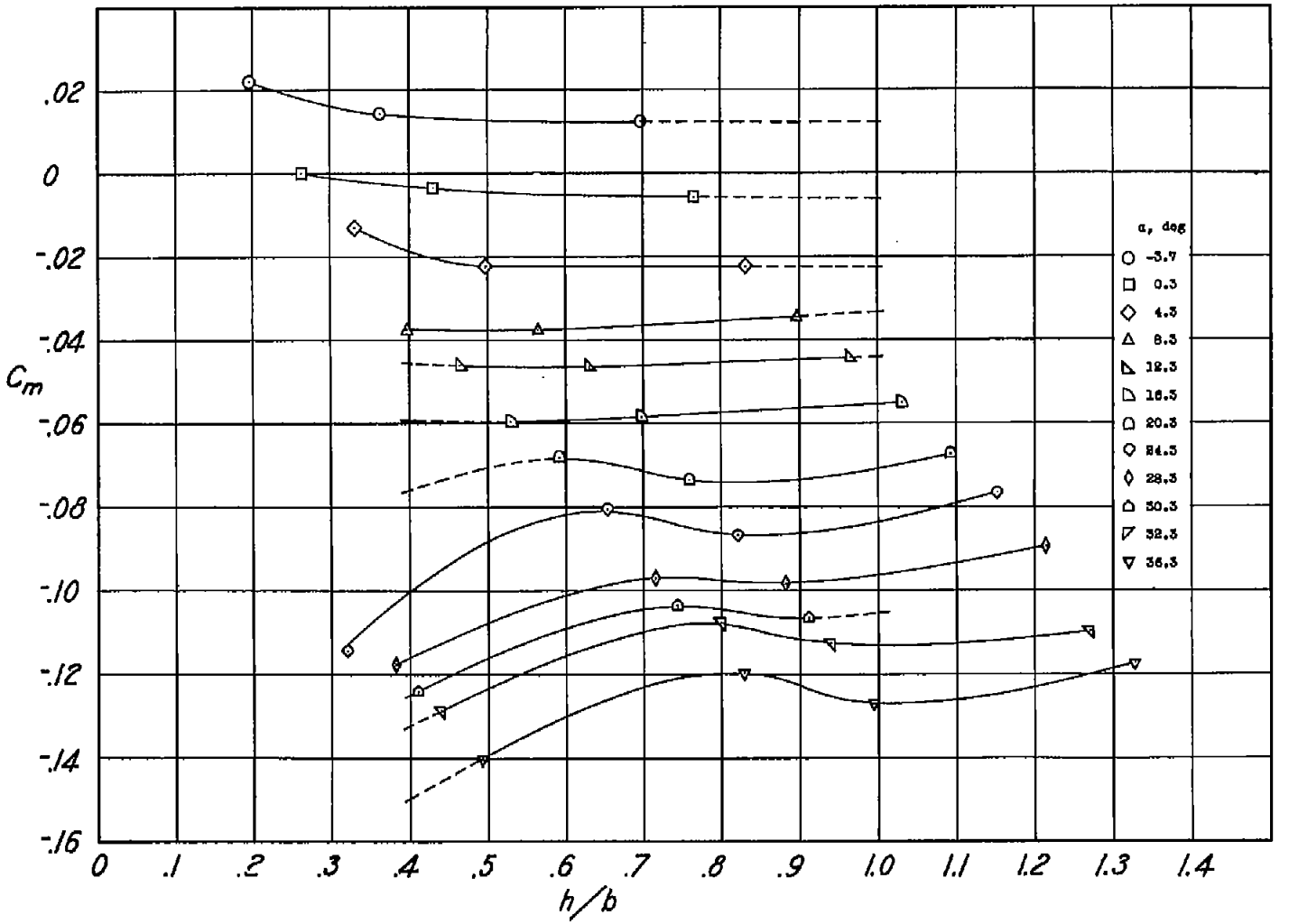

(c) Pitching-moment coefficient.

Figure 5.- Continued.

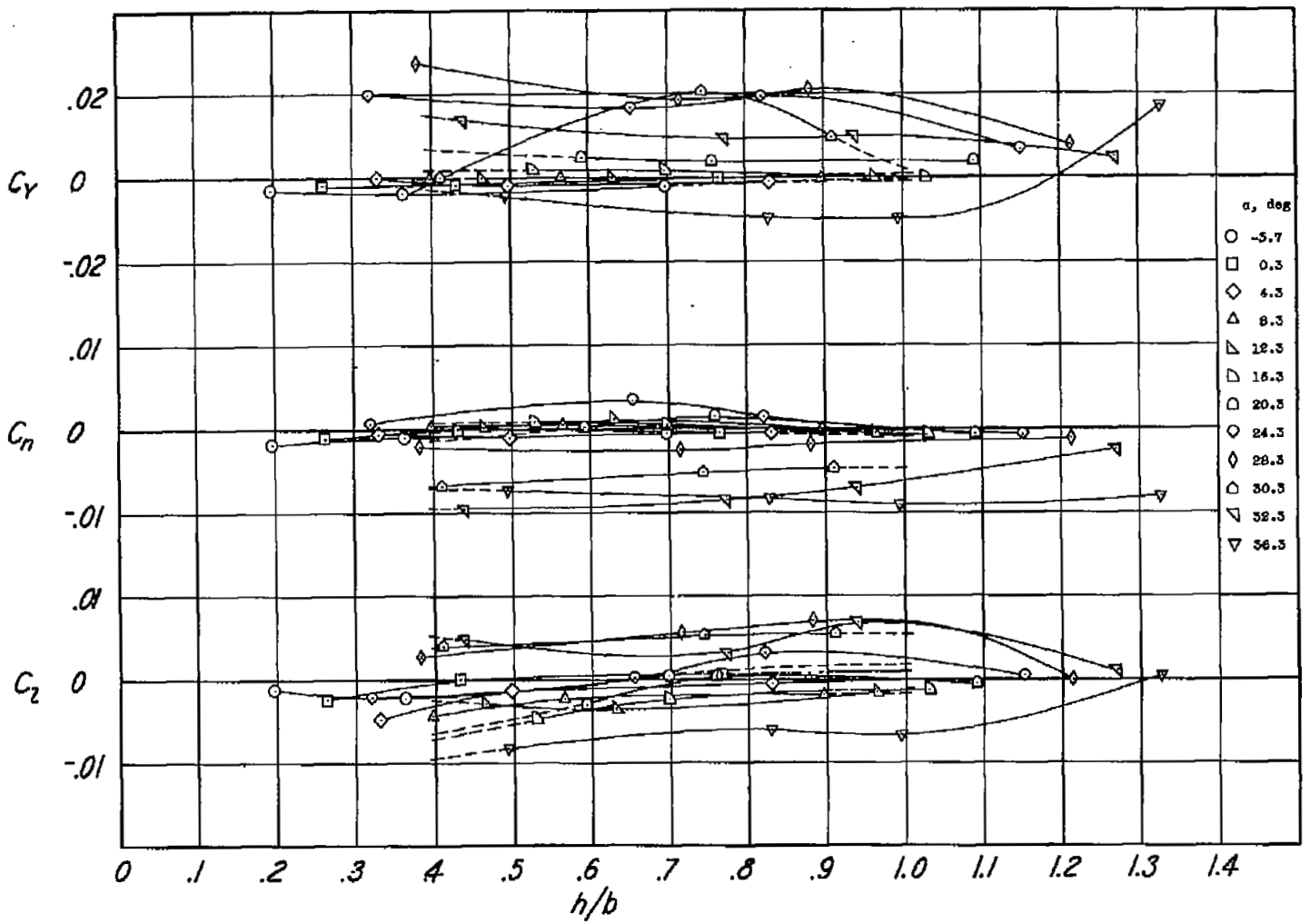

(d) Lateral-force, yawing-moment, and rolling-moment coefficients.

Figure 5.- Continued.

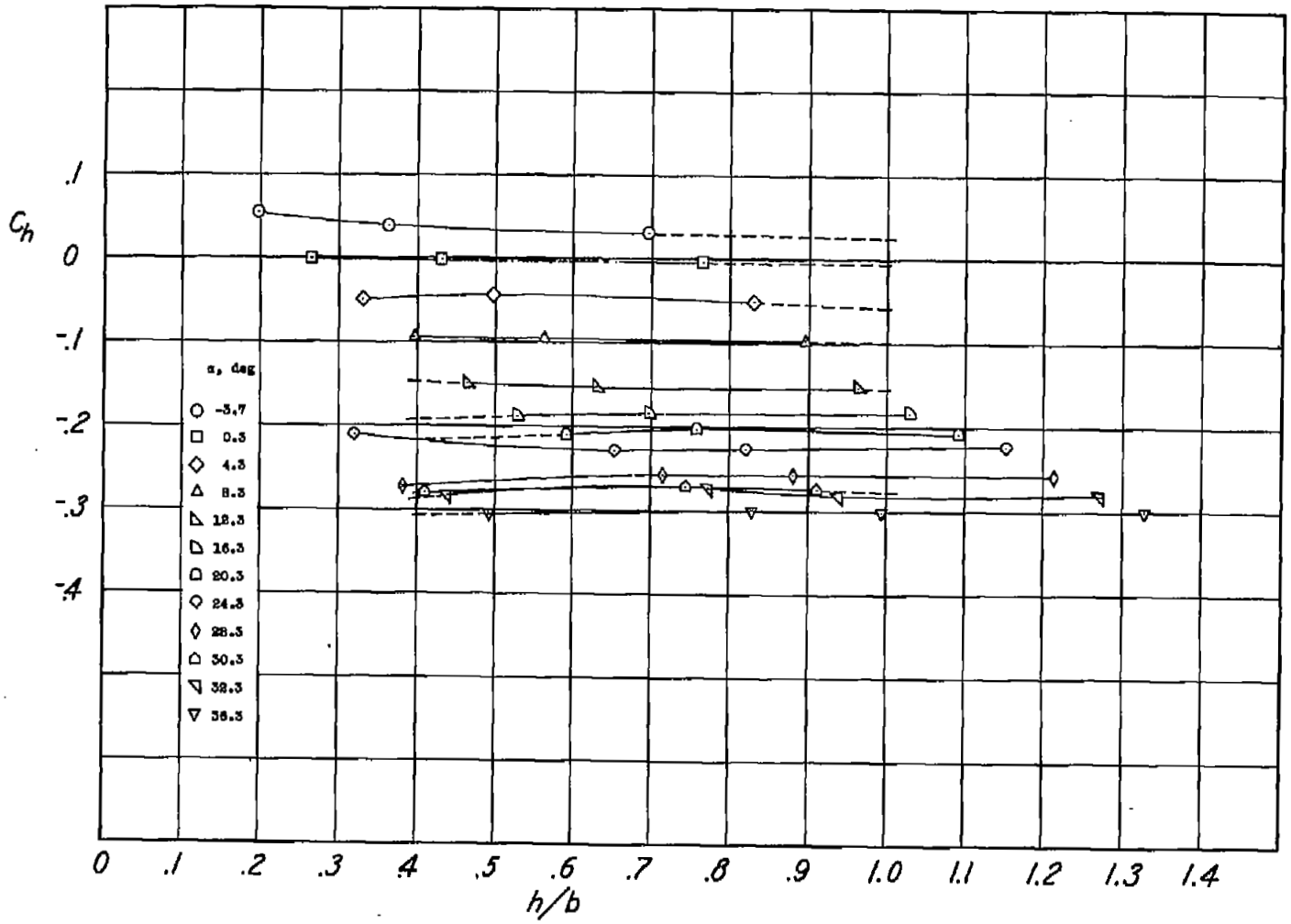

(e) Hinge-moment coefficient. (Horn-balance-type control.)

Figure 5.- Concluded.

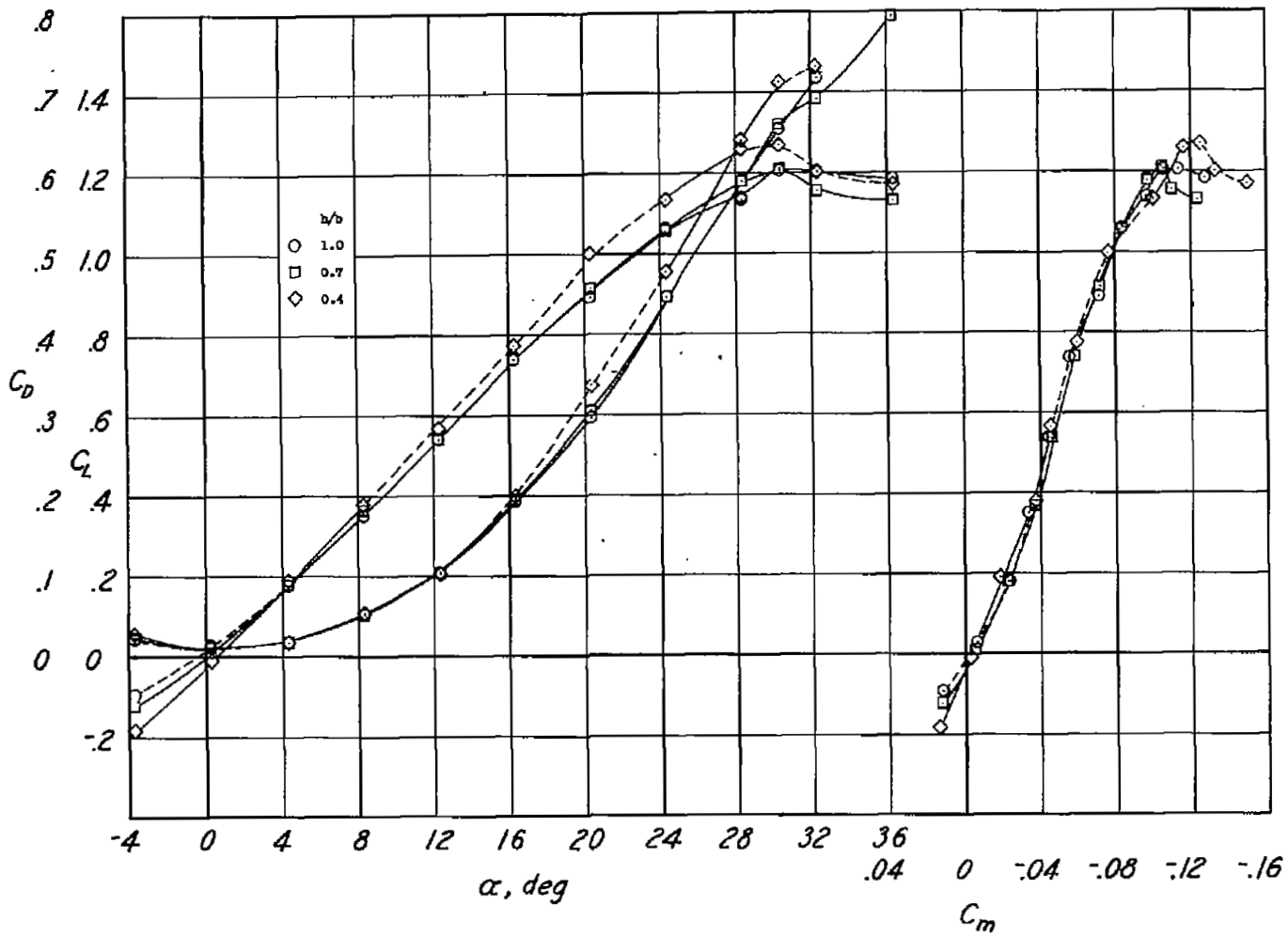

(a) $\delta_f = 0^\circ$.

Figure 6.- Longitudinal characteristics of the delta-wing model at several ground heights. $\delta_a = 0^\circ$.

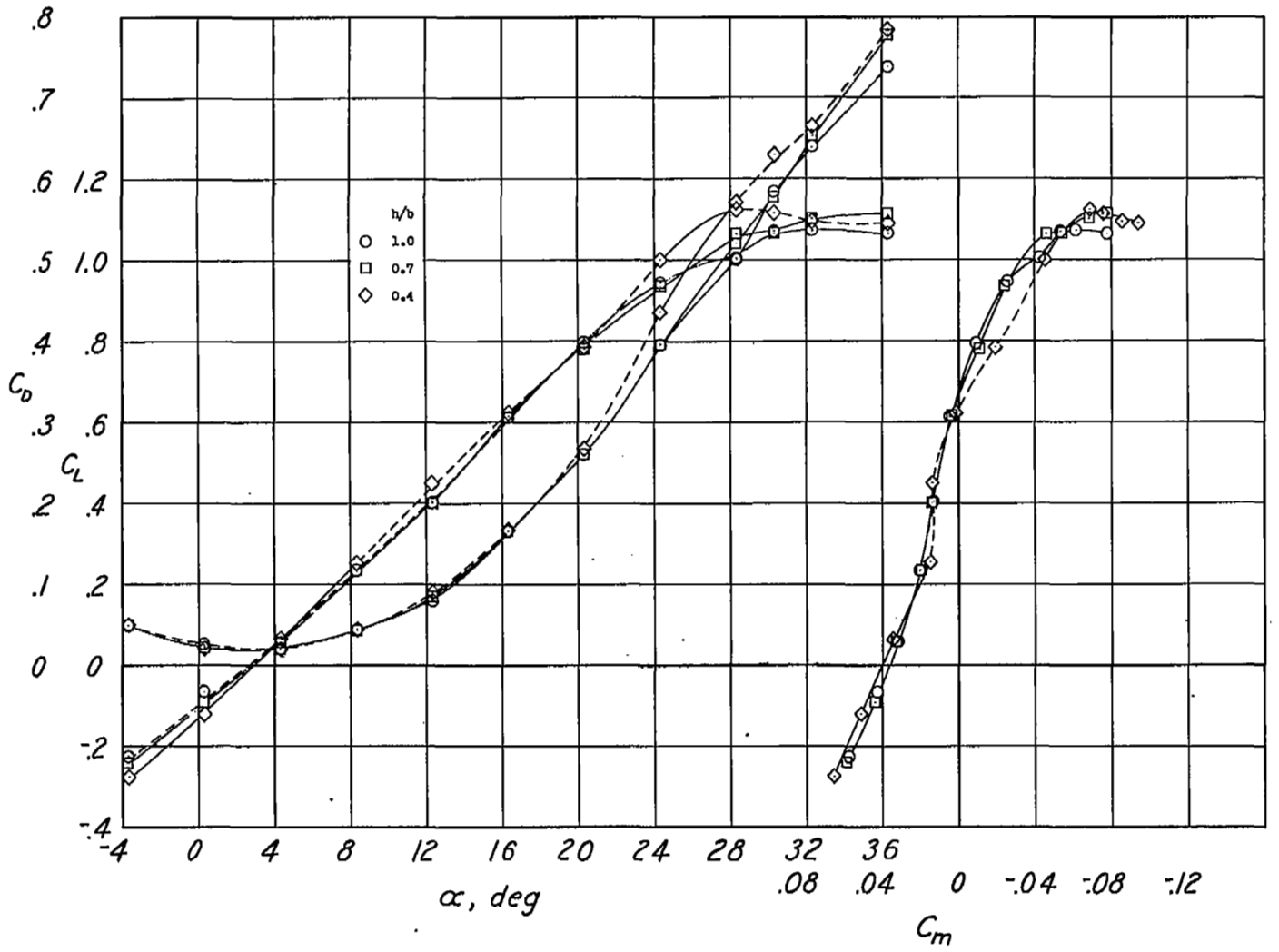

(b) $\delta_f = -10^\circ$.

Figure 6.- Continued.

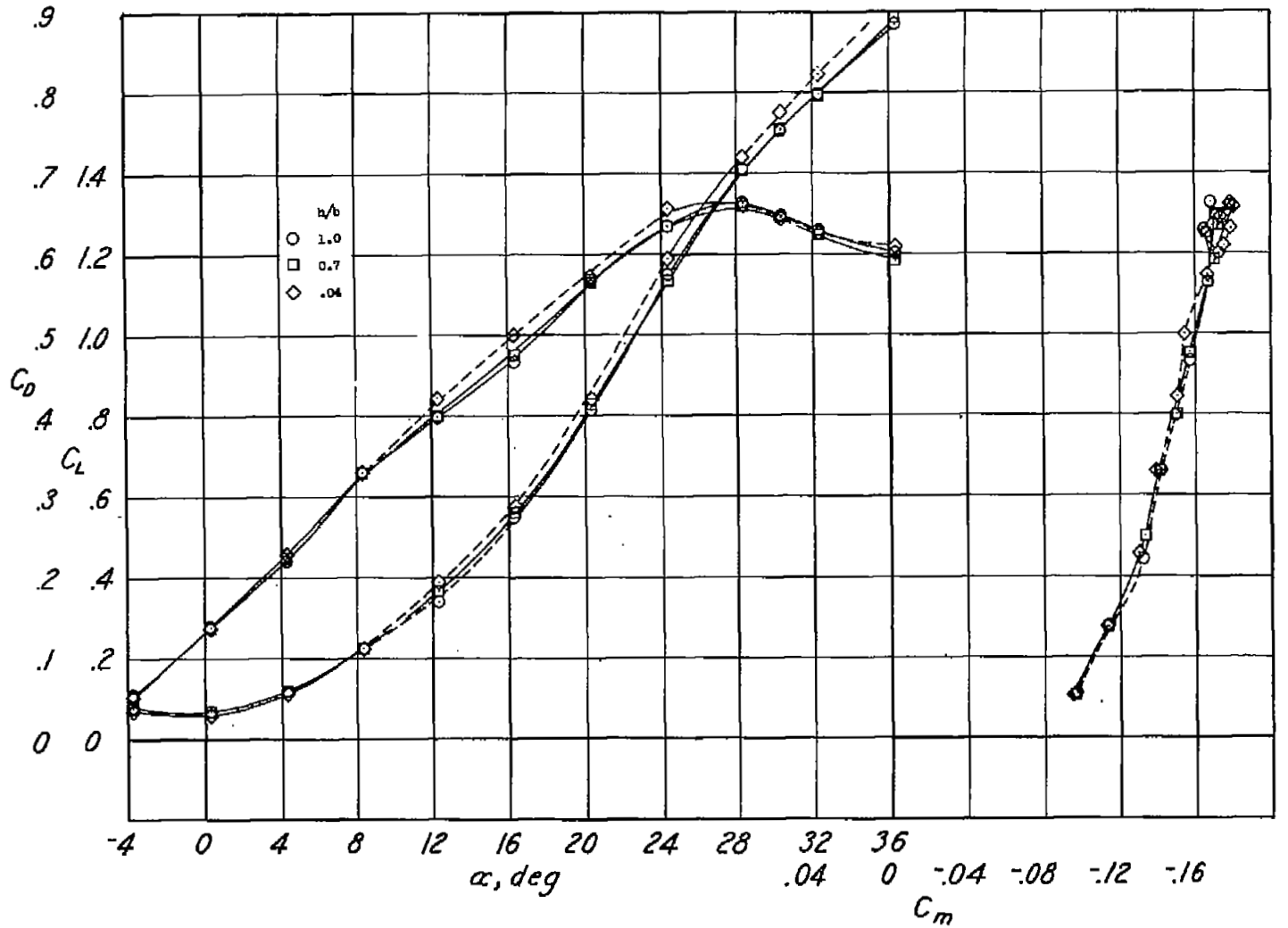

(c) $\delta_f = 20^\circ$.

Figure 6.- Continued.

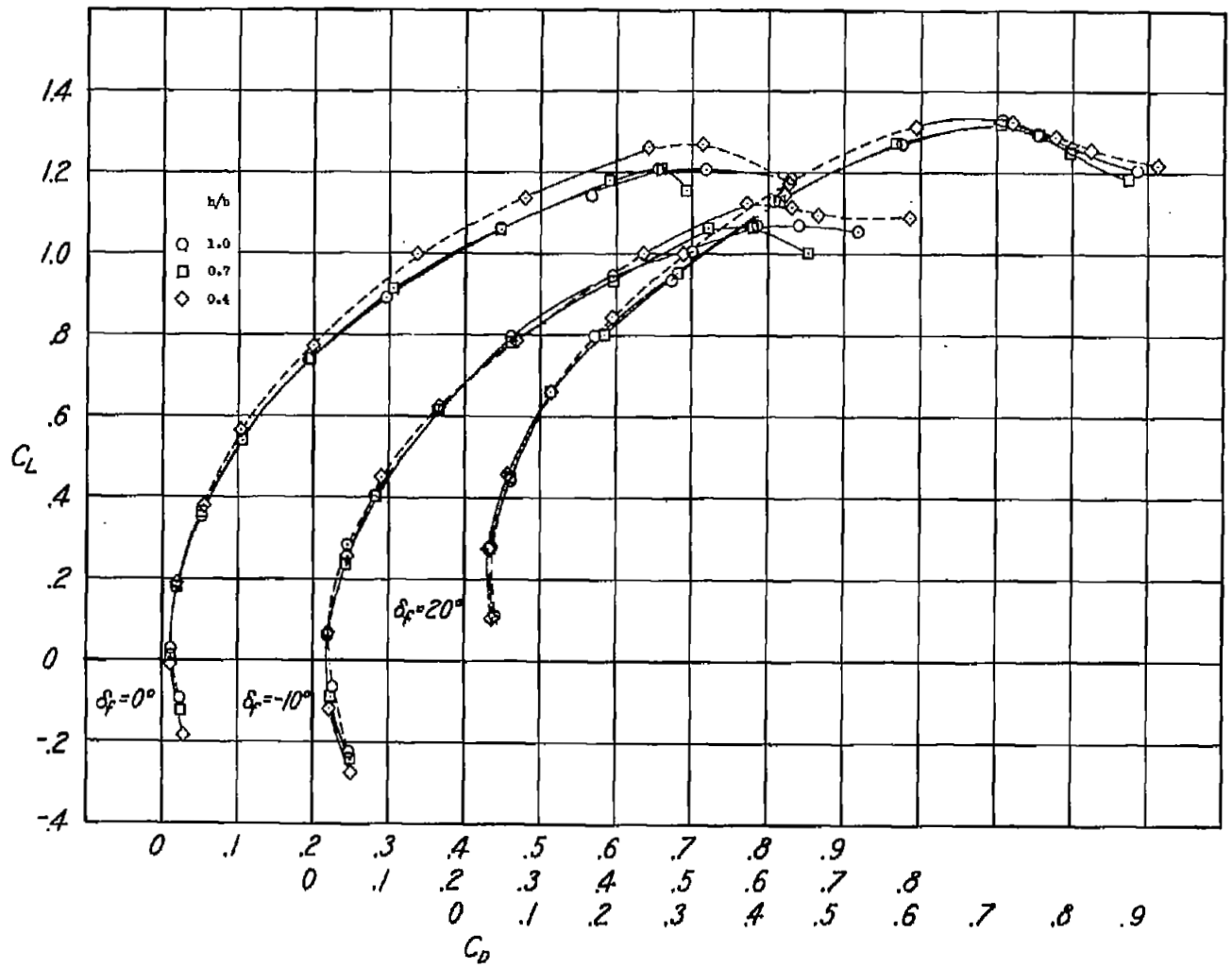

(d) Drag characteristics.

Figure 6.- Concluded.

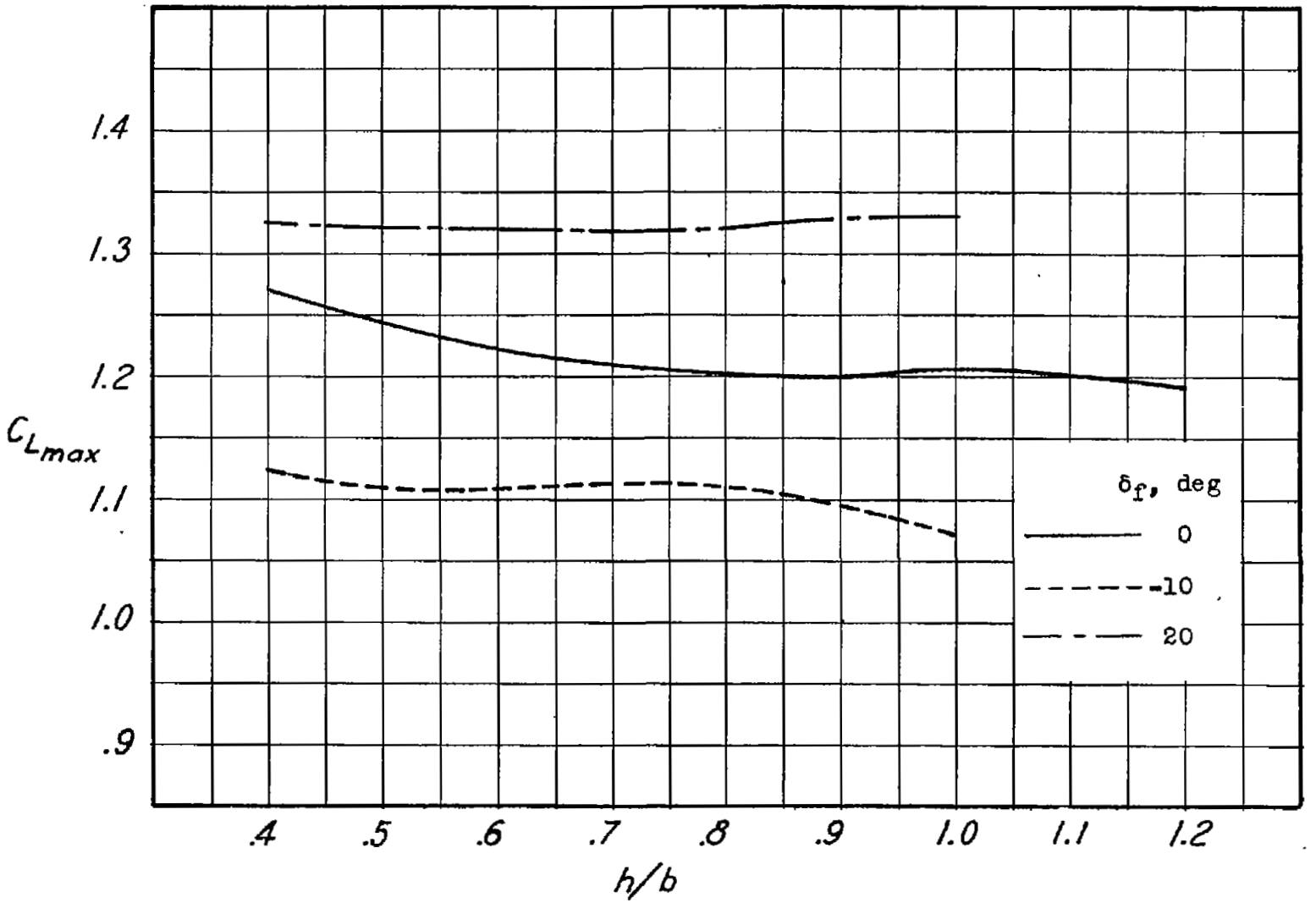

Figure 7.- Variation of maximum lift coefficient with height span ratio for three flap deflections. $\delta_a = 0^o$.

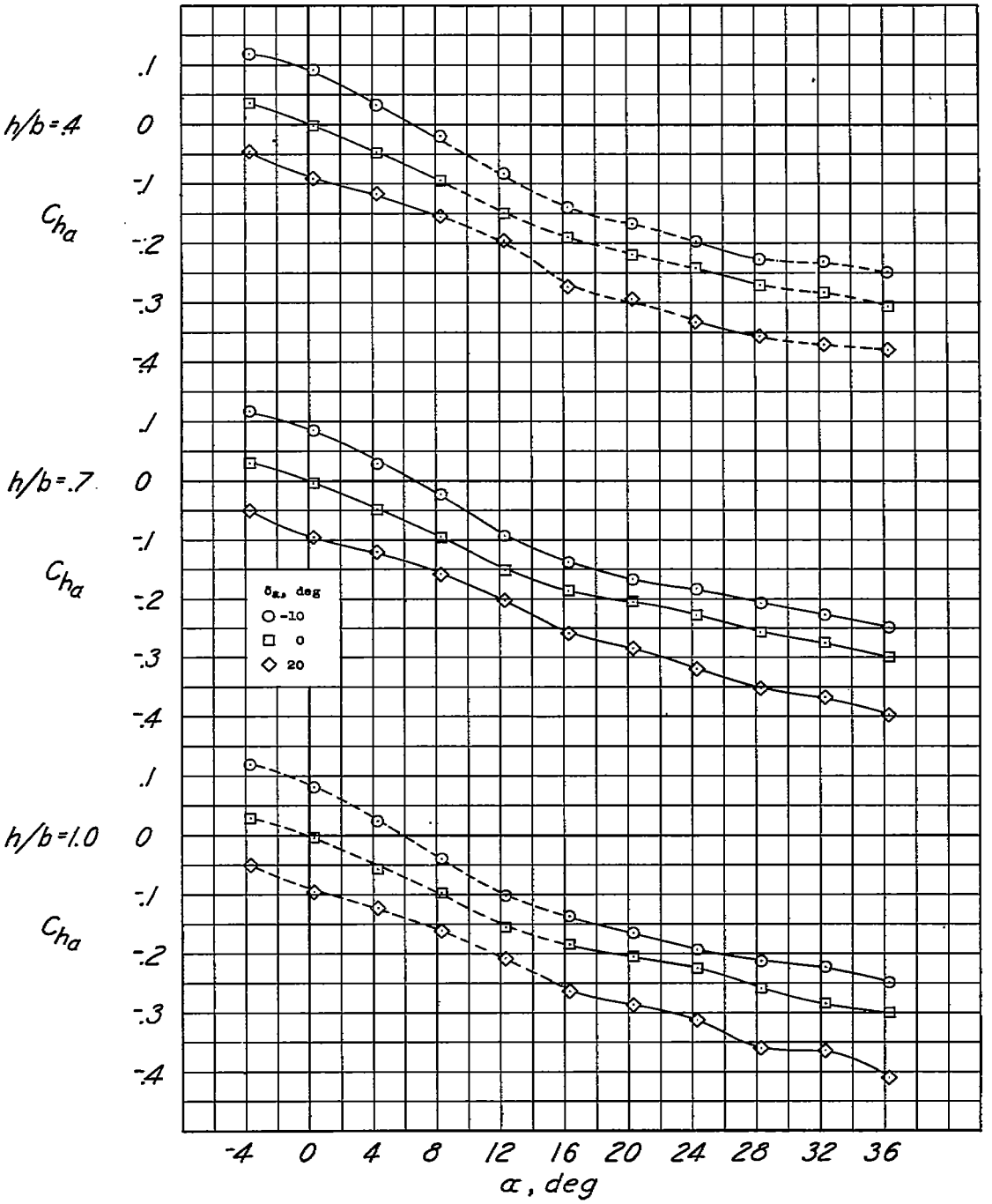

(a) $\delta_f = 0^\circ$.

Figure 8.- Variation of aileron hinge-moment coefficient with angle of attack at three ground heights.

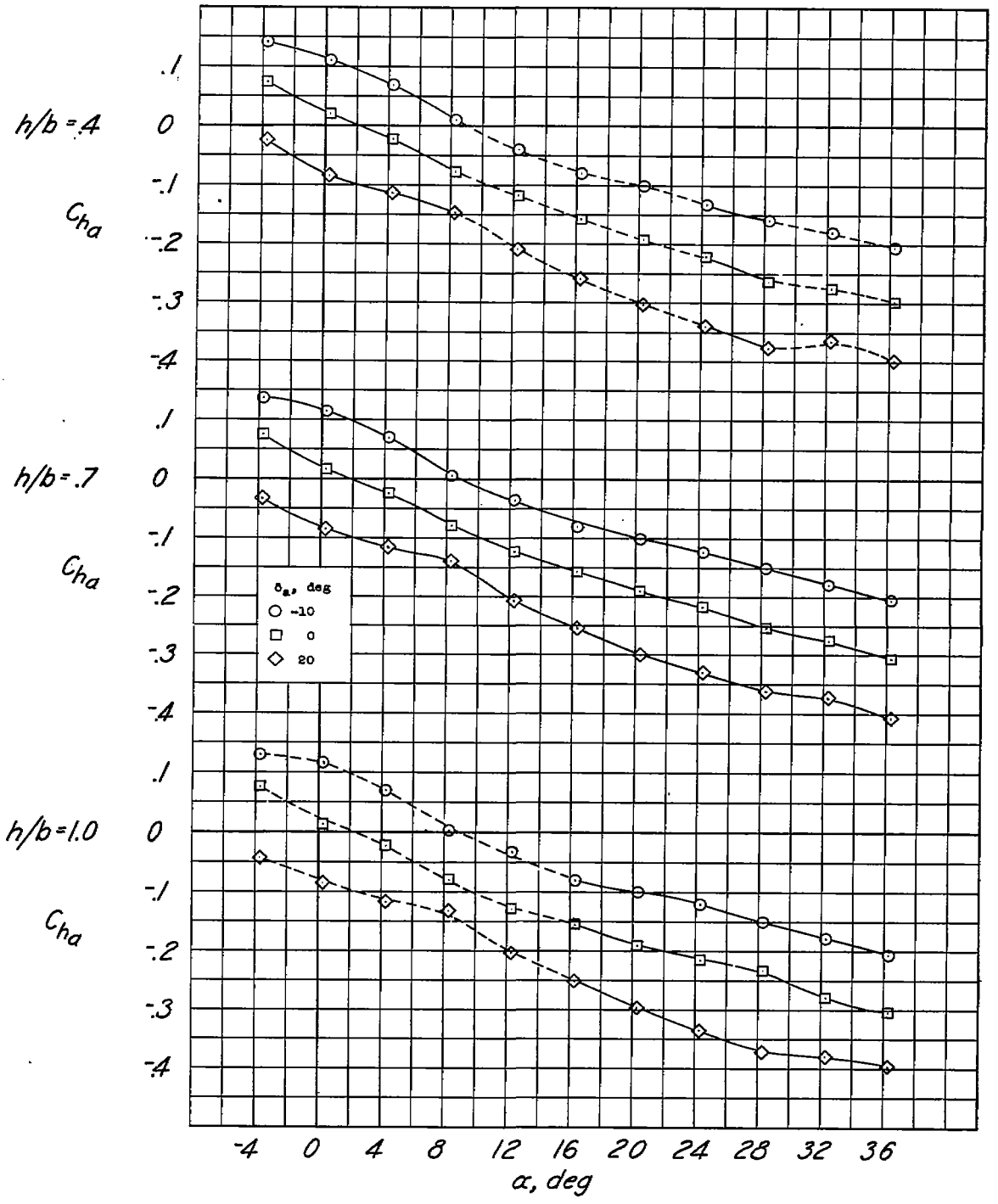

(b) $\delta_f = -10^\circ$.

Figure 8.- Continued.

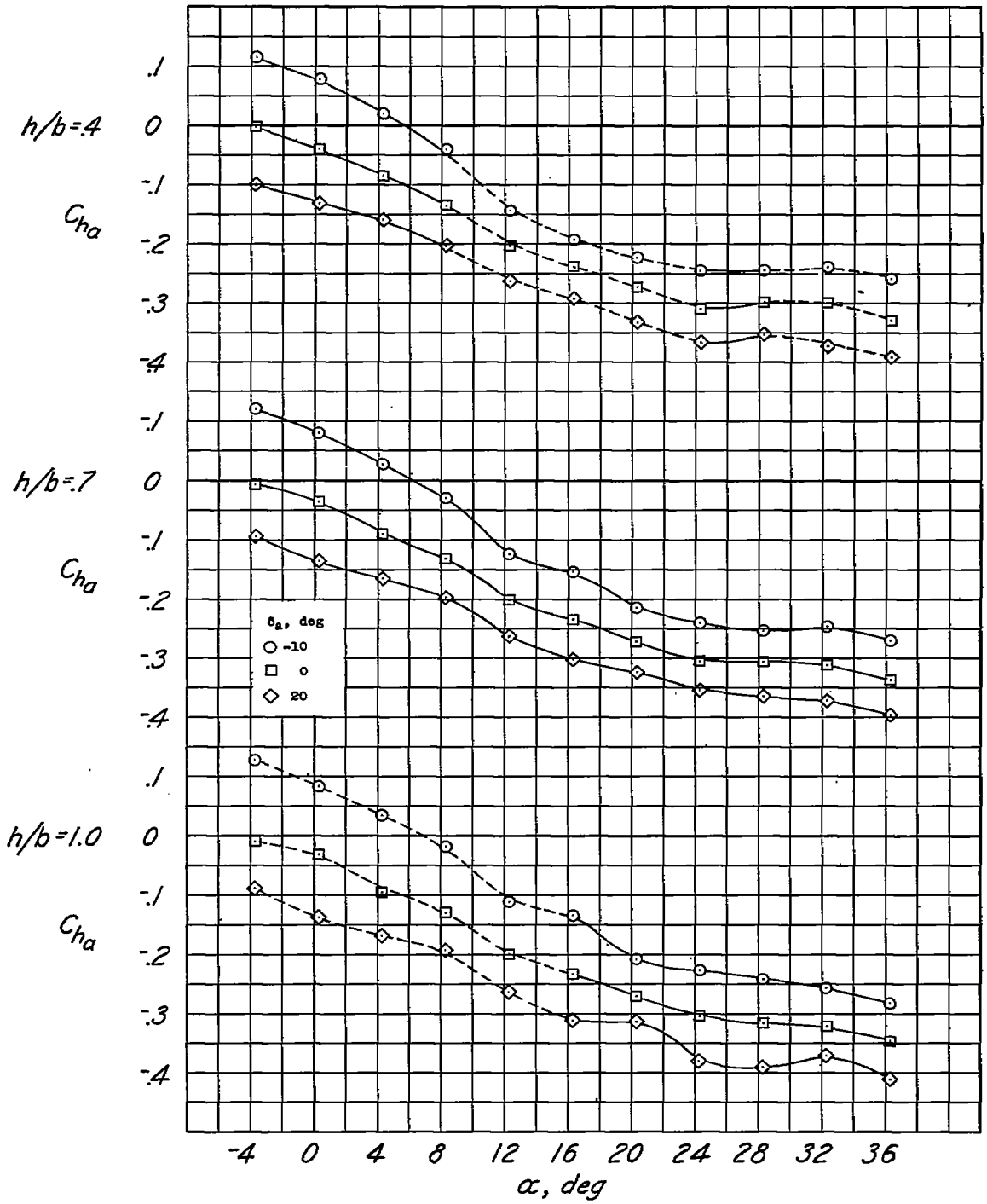

(c) $\delta_f = 20^\circ$.

Figure 8.- Concluded.

[redacted]

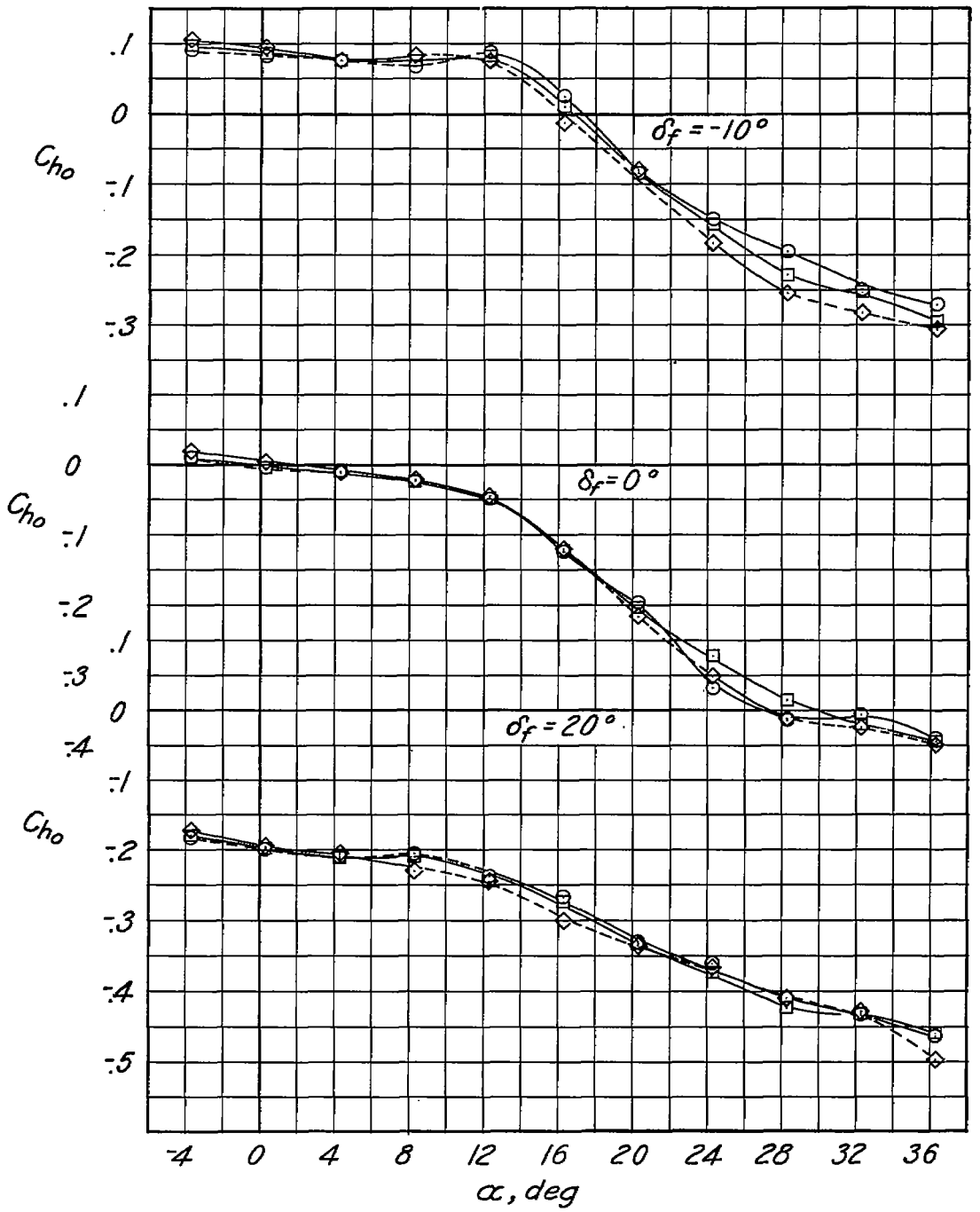

(a) Outboard flap segment.

Figure 9.- Variation of flap segment and complete flap hinge-moment coefficient with angle of attack. $\delta_a = 0°$.

[redacted]

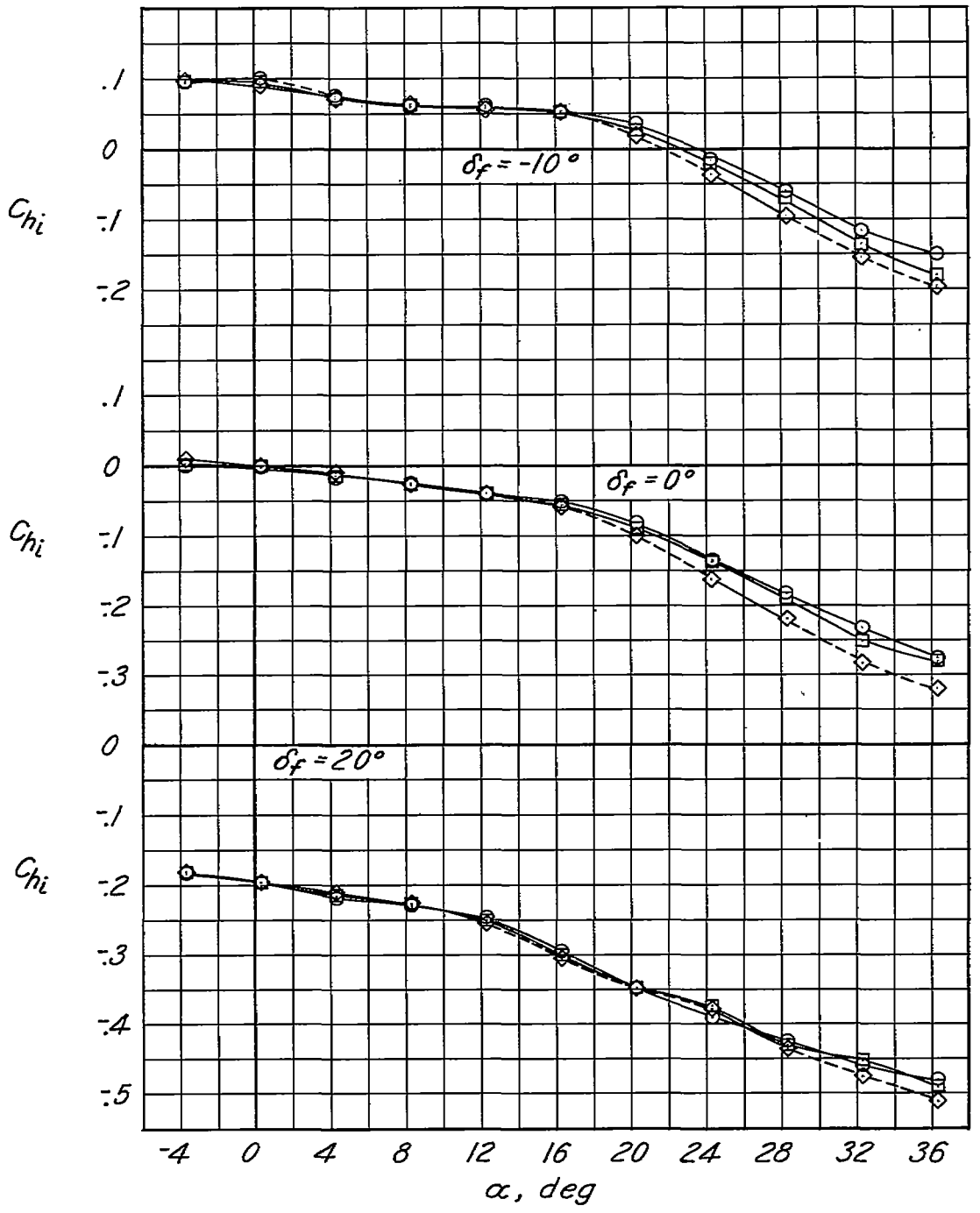

(b) Inboard flap segment.

Figure 9.- Continued.

[redacted]

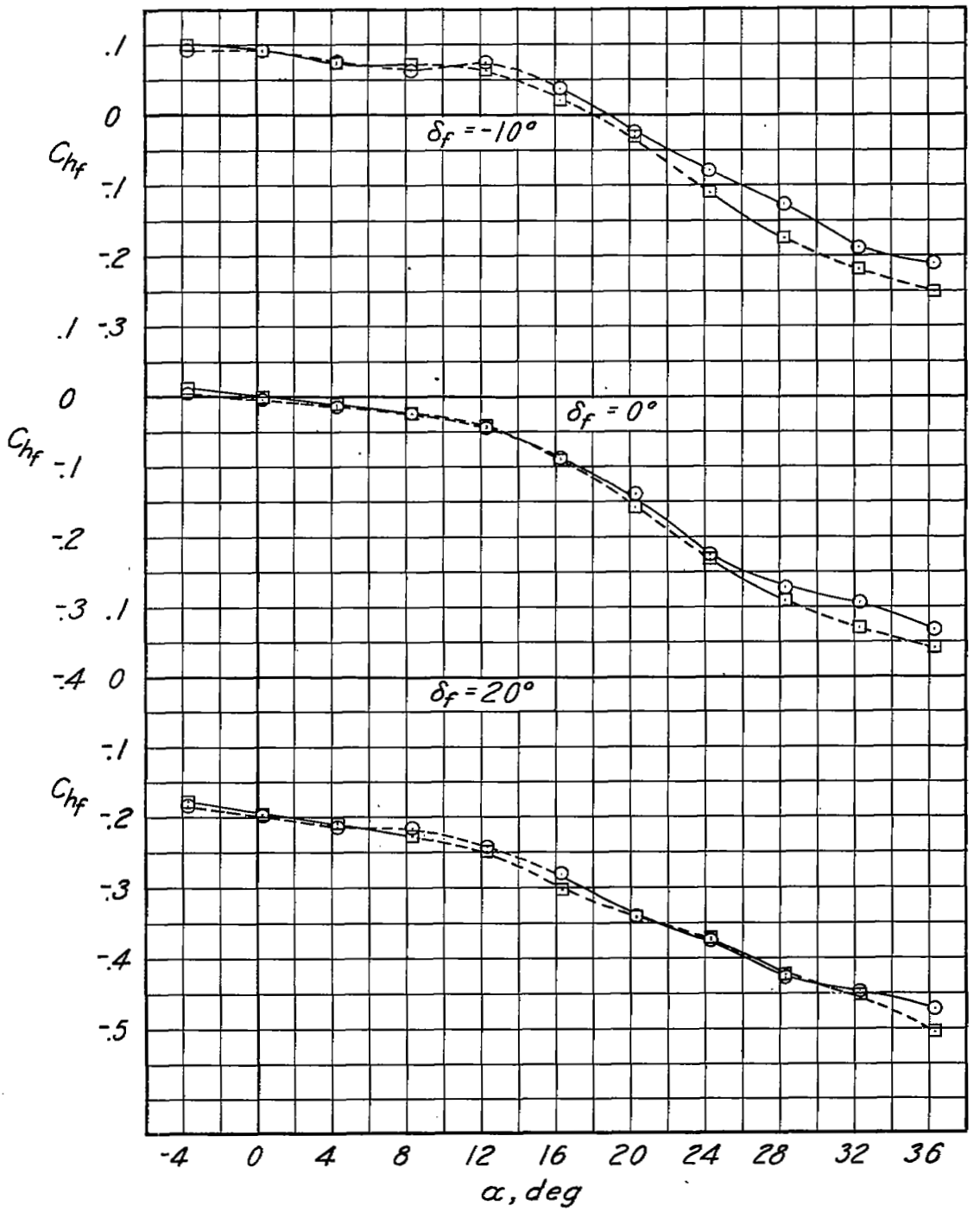

(c) Complete flap.

Figure 9.- Concluded.

[redacted]

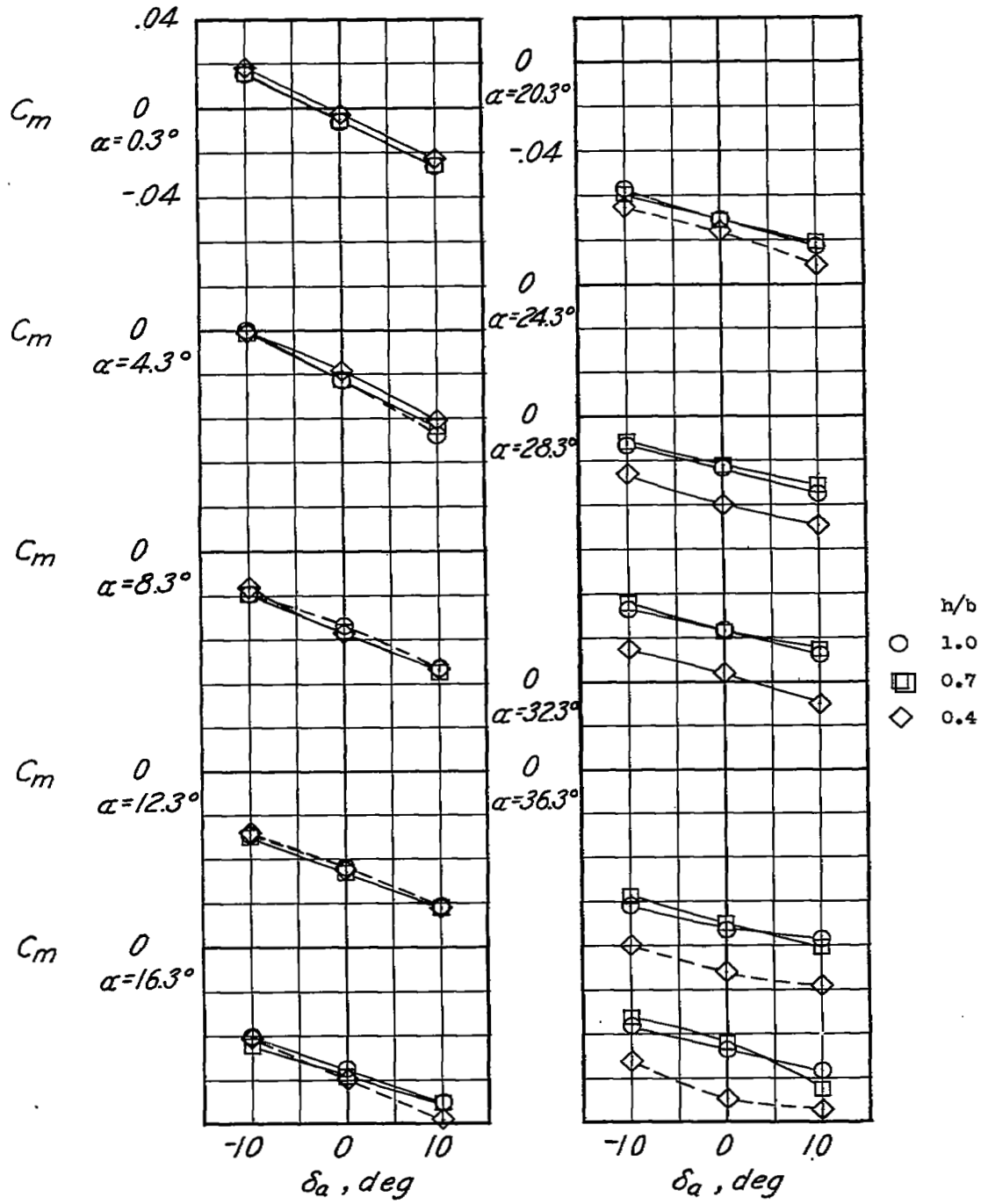

(a) $\delta_f = 0°$.

Figure 10.- Variation of pitching-moment coefficient with aileron deflection at three ground heights.

[redacted]

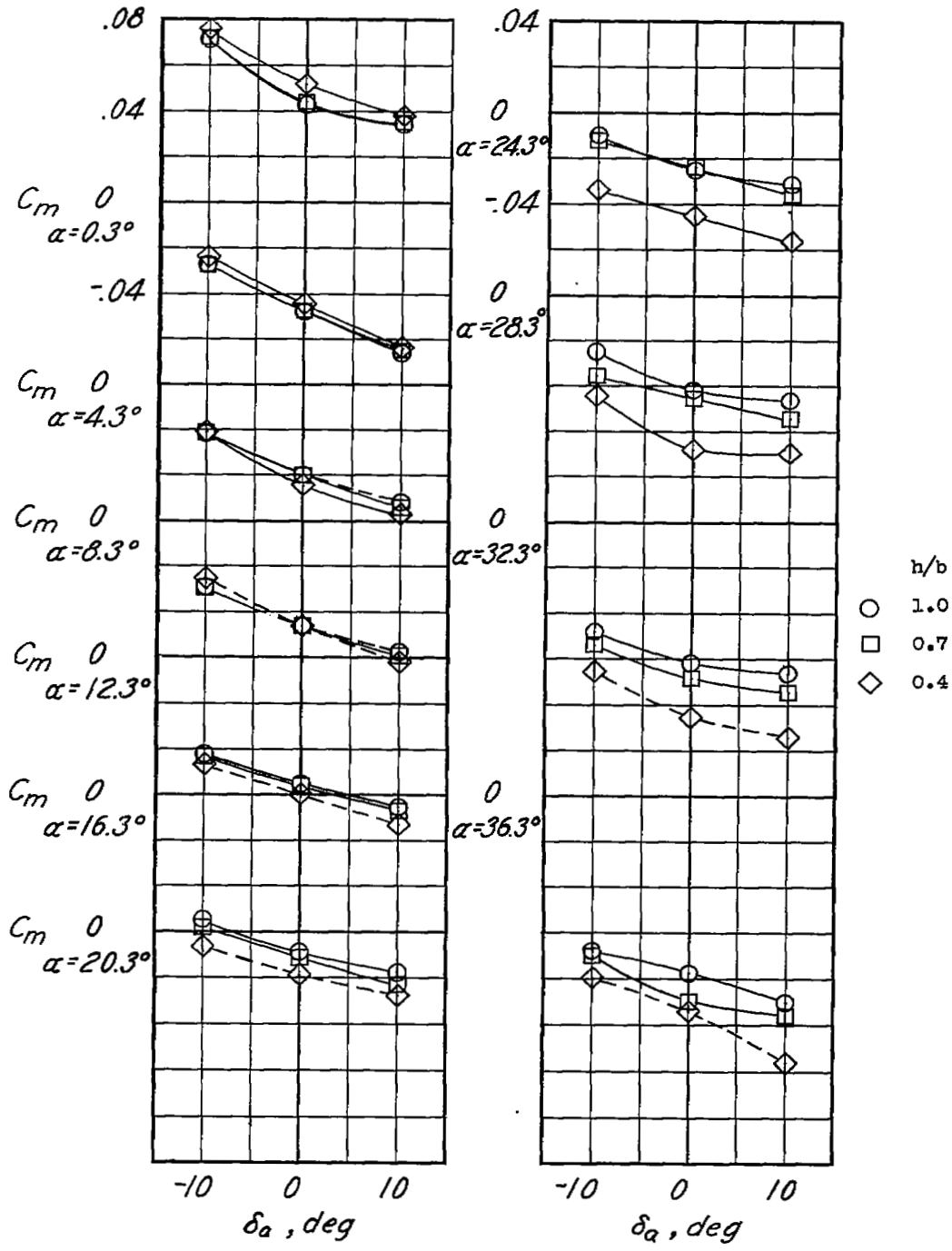

(b) $\delta_f = -10^\circ$.

Figure 10.- Continued.

[redacted]

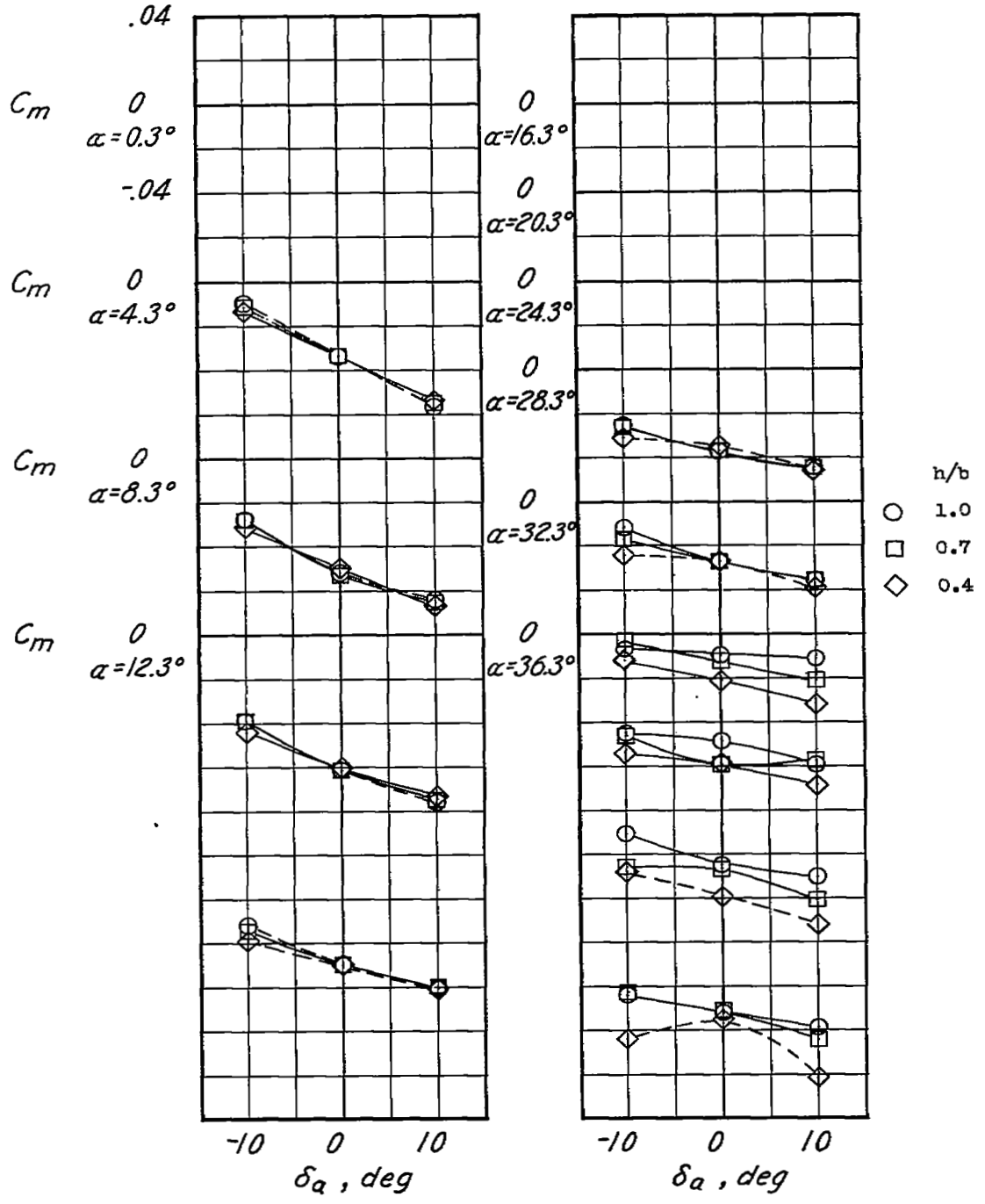

(c) $\delta_f = 20^\circ$.

Figure 10.- Concluded.

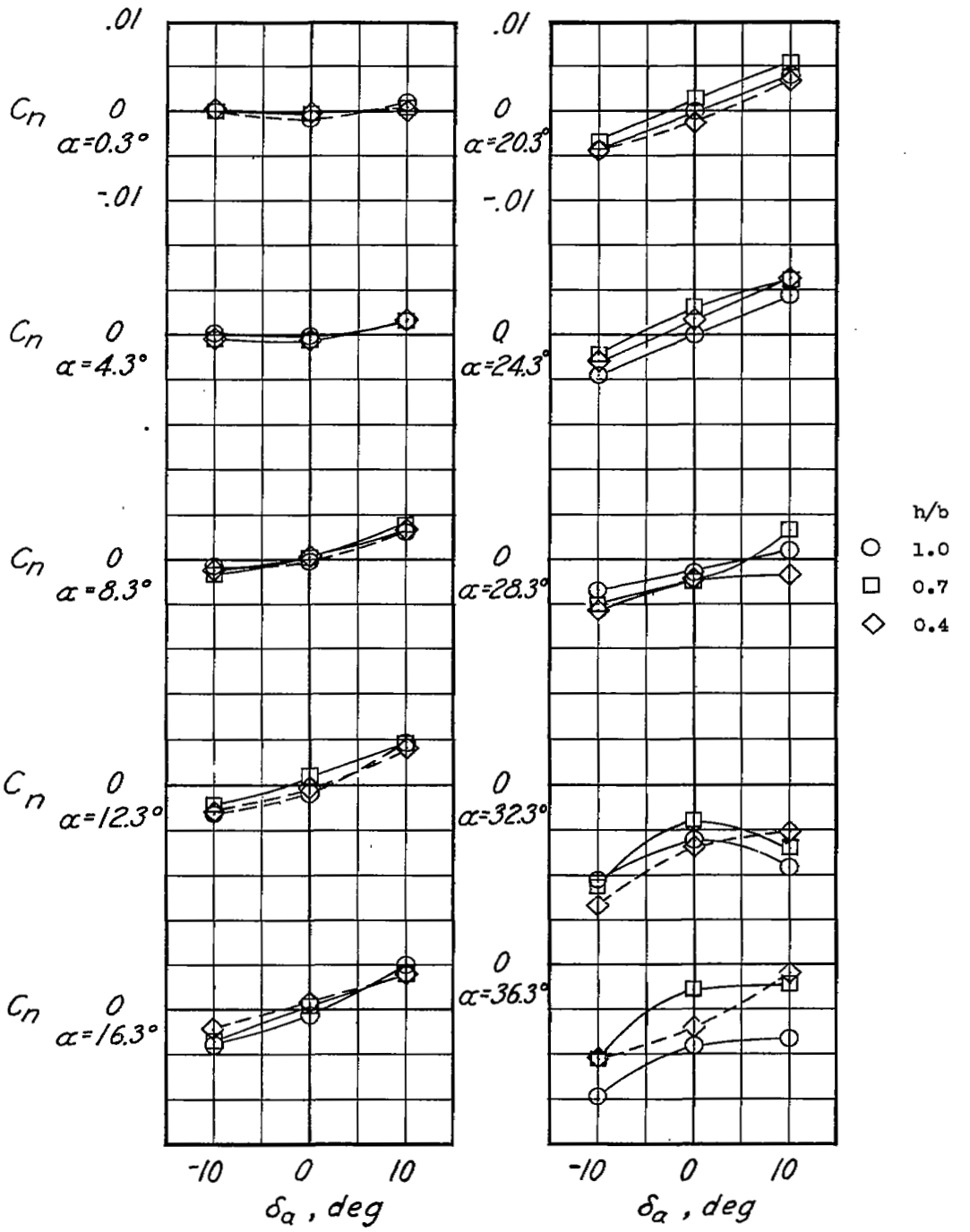

(a) $\delta_f = 0°$.

Figure 11.- Variation of yawing-moment coefficient with aileron deflection at three ground heights.

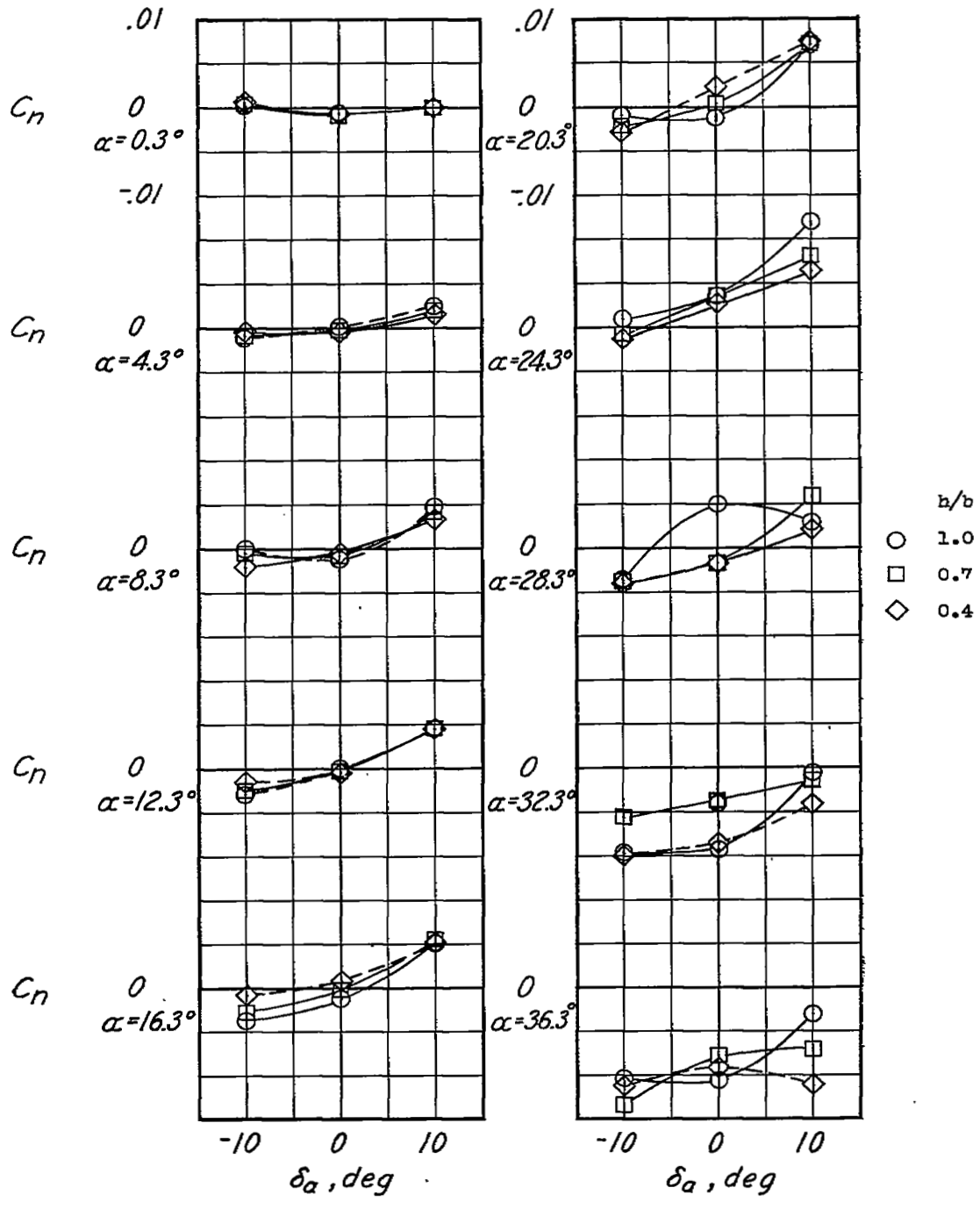

(b) $\delta_f = -10^\circ$.

Figure 11.- Continued.

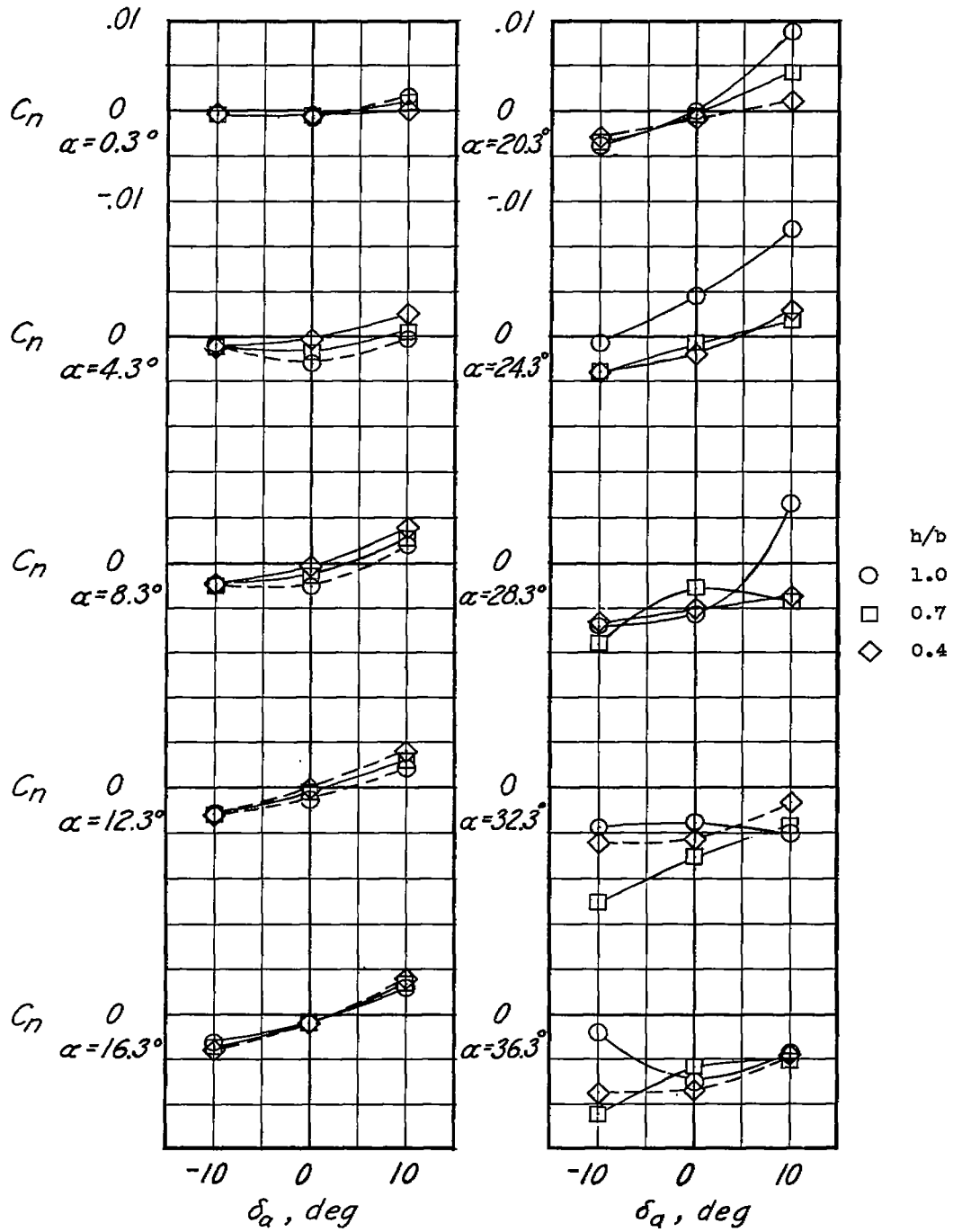

(c) $\delta_f = 20°$.

Figure 11.- Concluded.

[redacted]

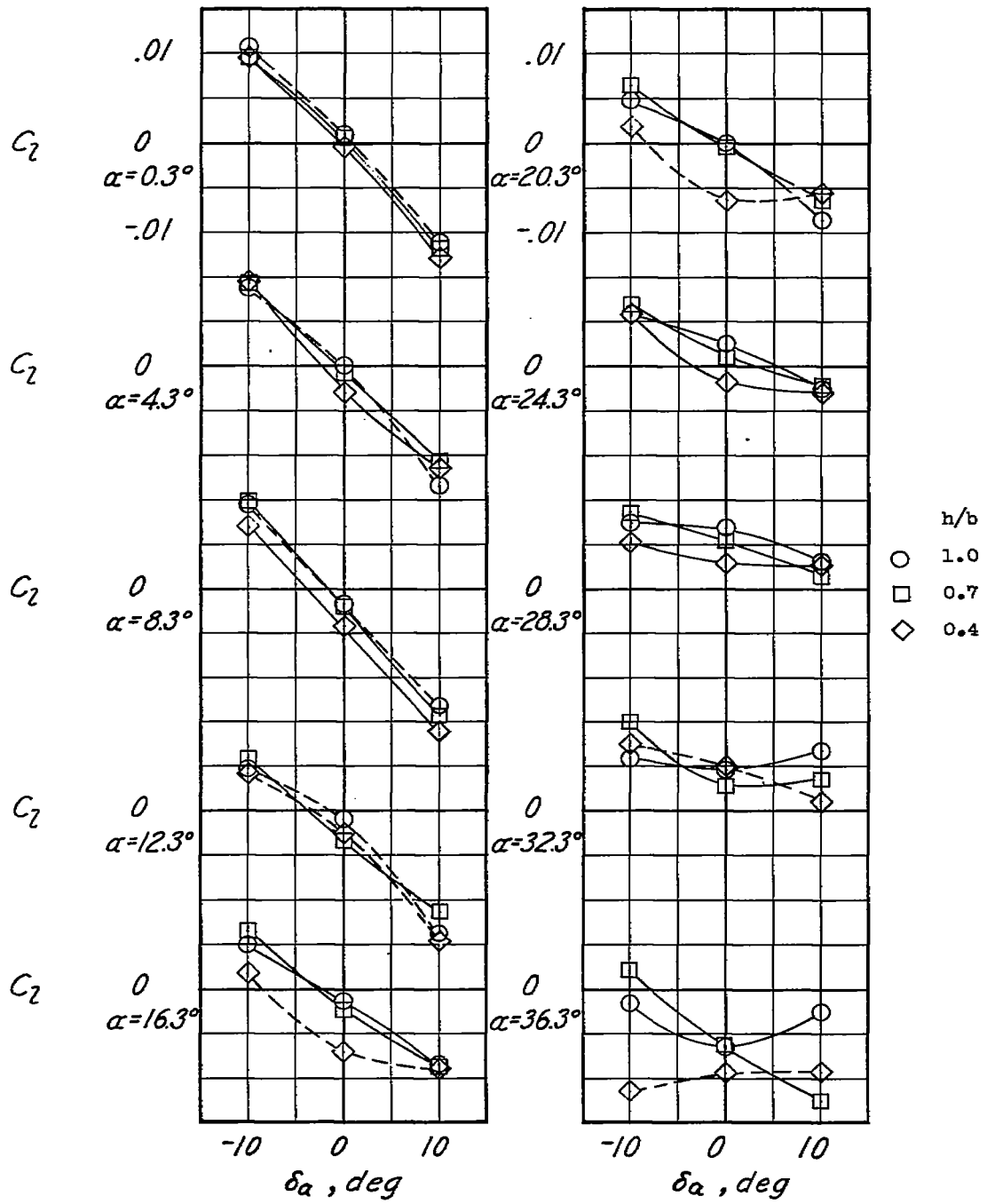

(a) $\delta_f = 0^\circ$.

Figure 12.- Variation of rolling-moment coefficient with aileron deflection at three ground heights.

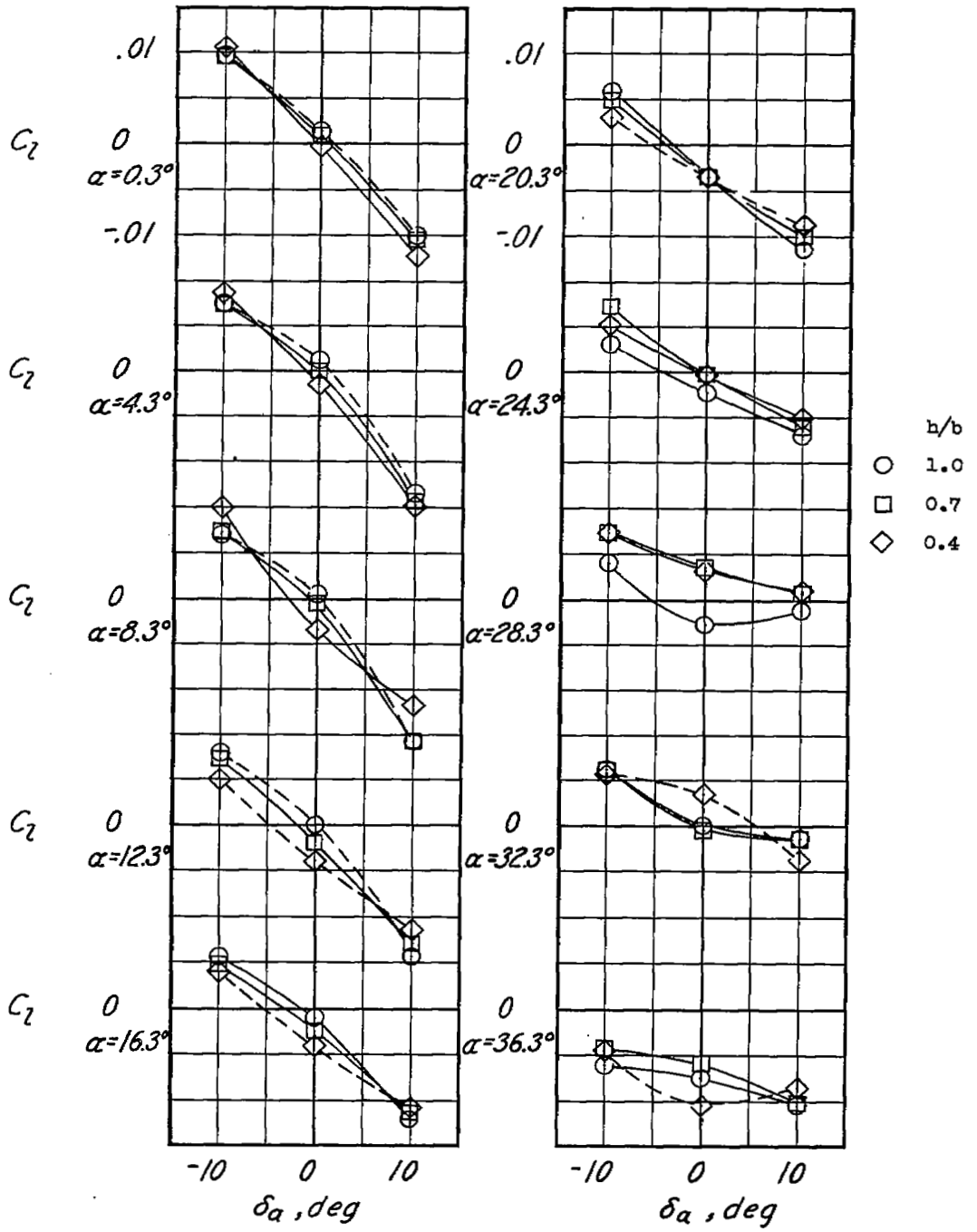

(b) $\delta_f = -10^\circ$.

Figure 12.- Continued.

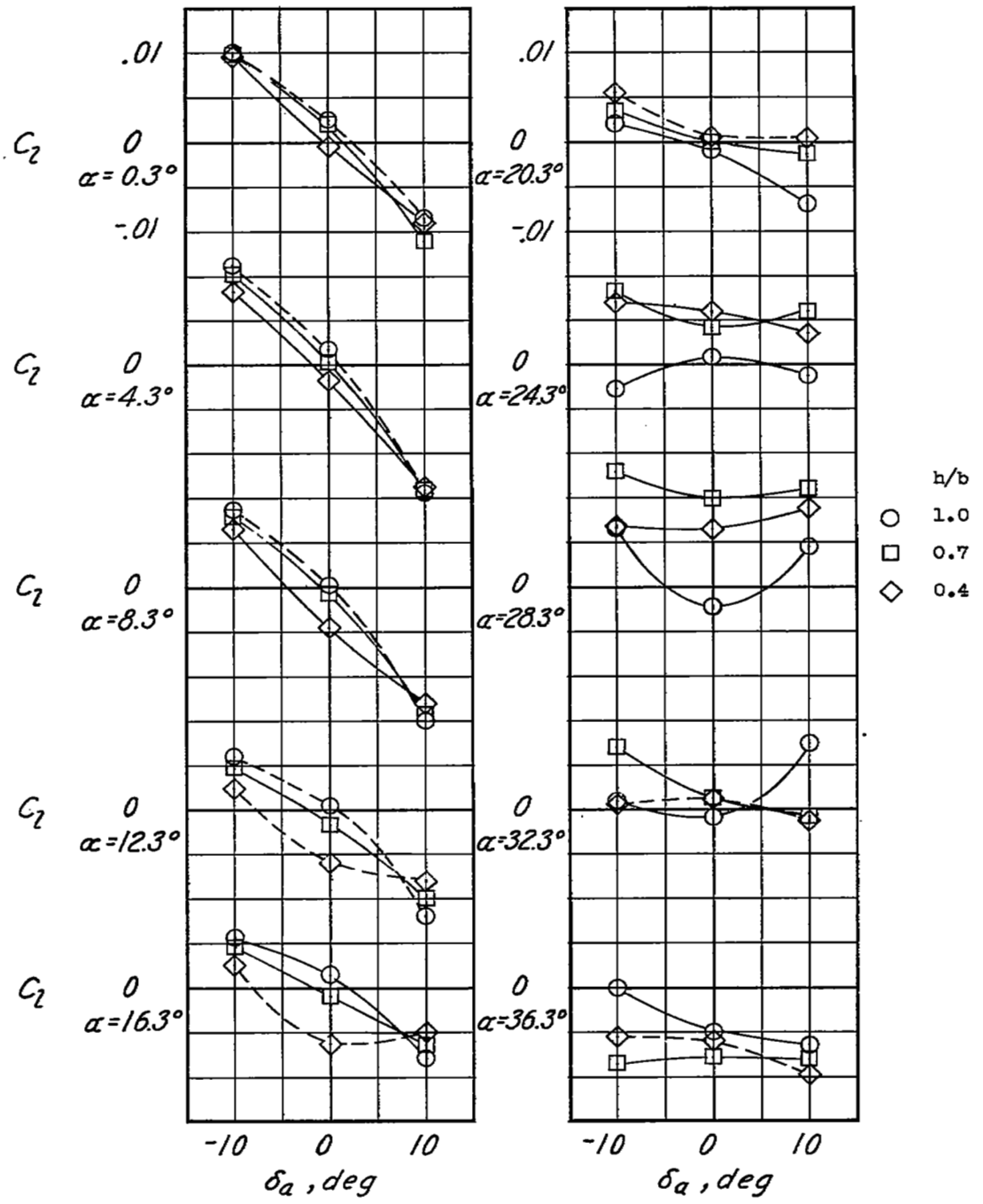

(c) $\delta_f = 20°$.

Figure 12.- Concluded.

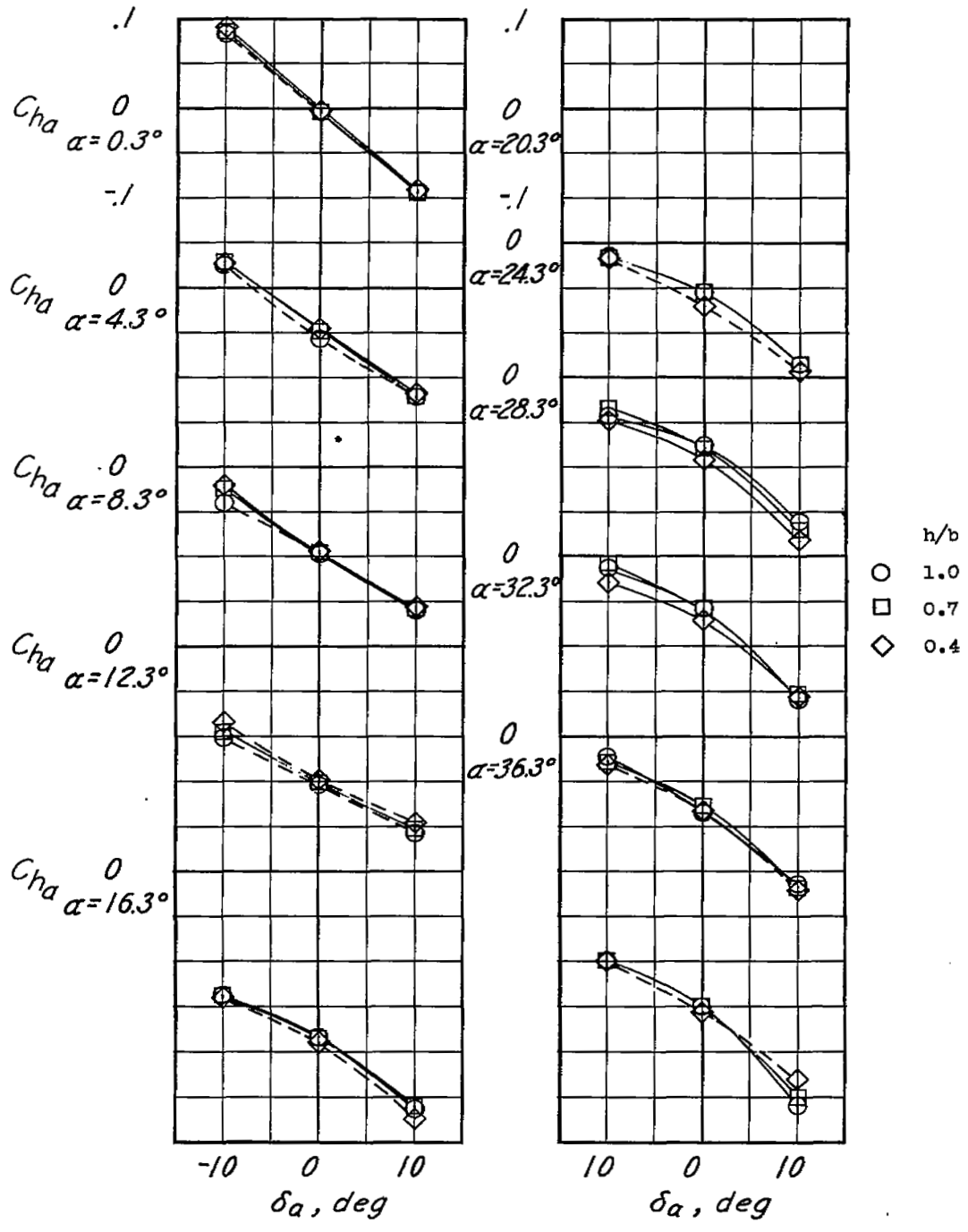

(a) $\delta_f = 0^\circ$.

Figure 13.- Variation of hinge-moment coefficient with aileron deflection at three ground heights.

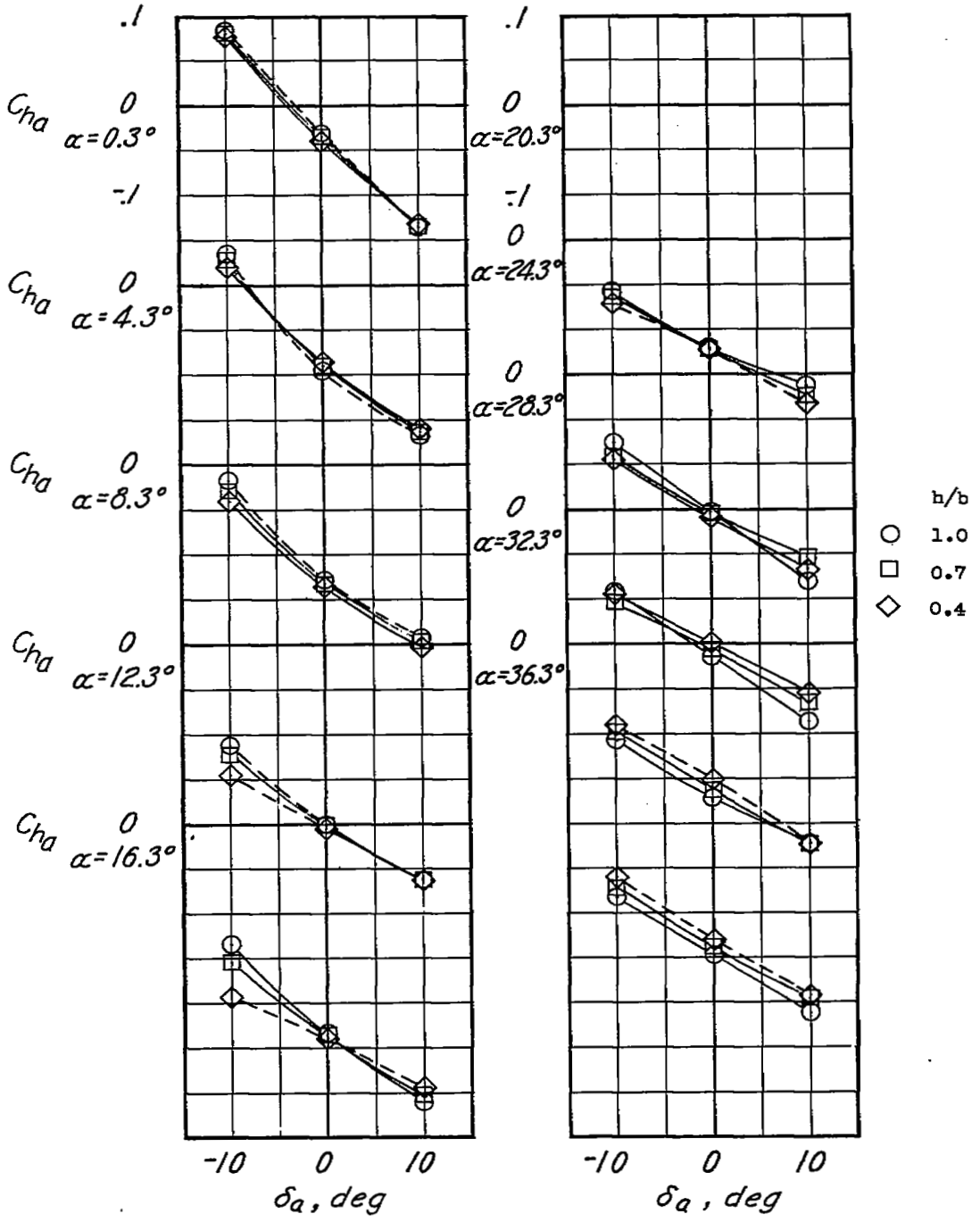

(b) $\delta_f = -10^\circ$.

Figure 13.- Continued.

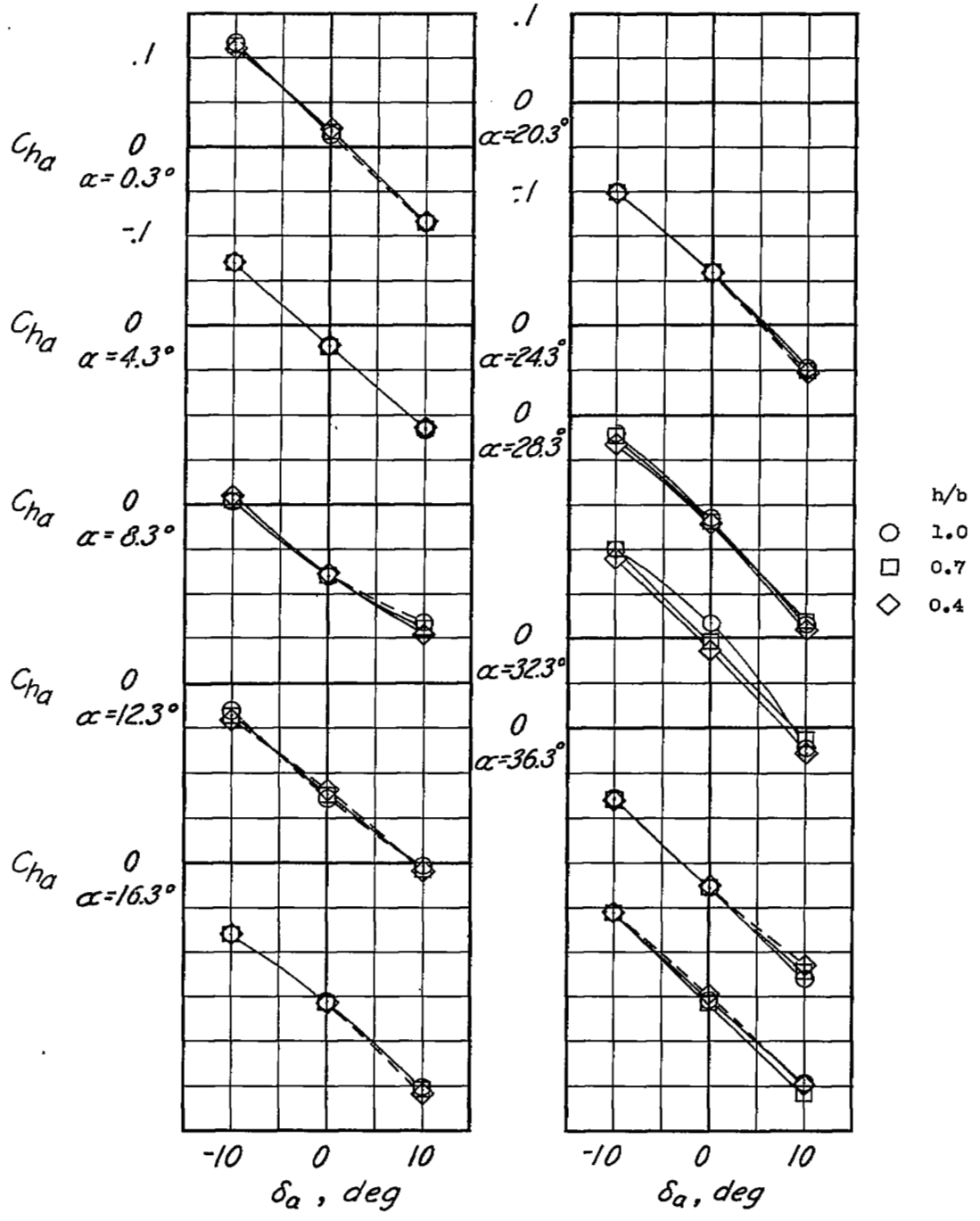

(c) $\delta_f = 20°$.

Figure 13.- Concluded.

[redacted]

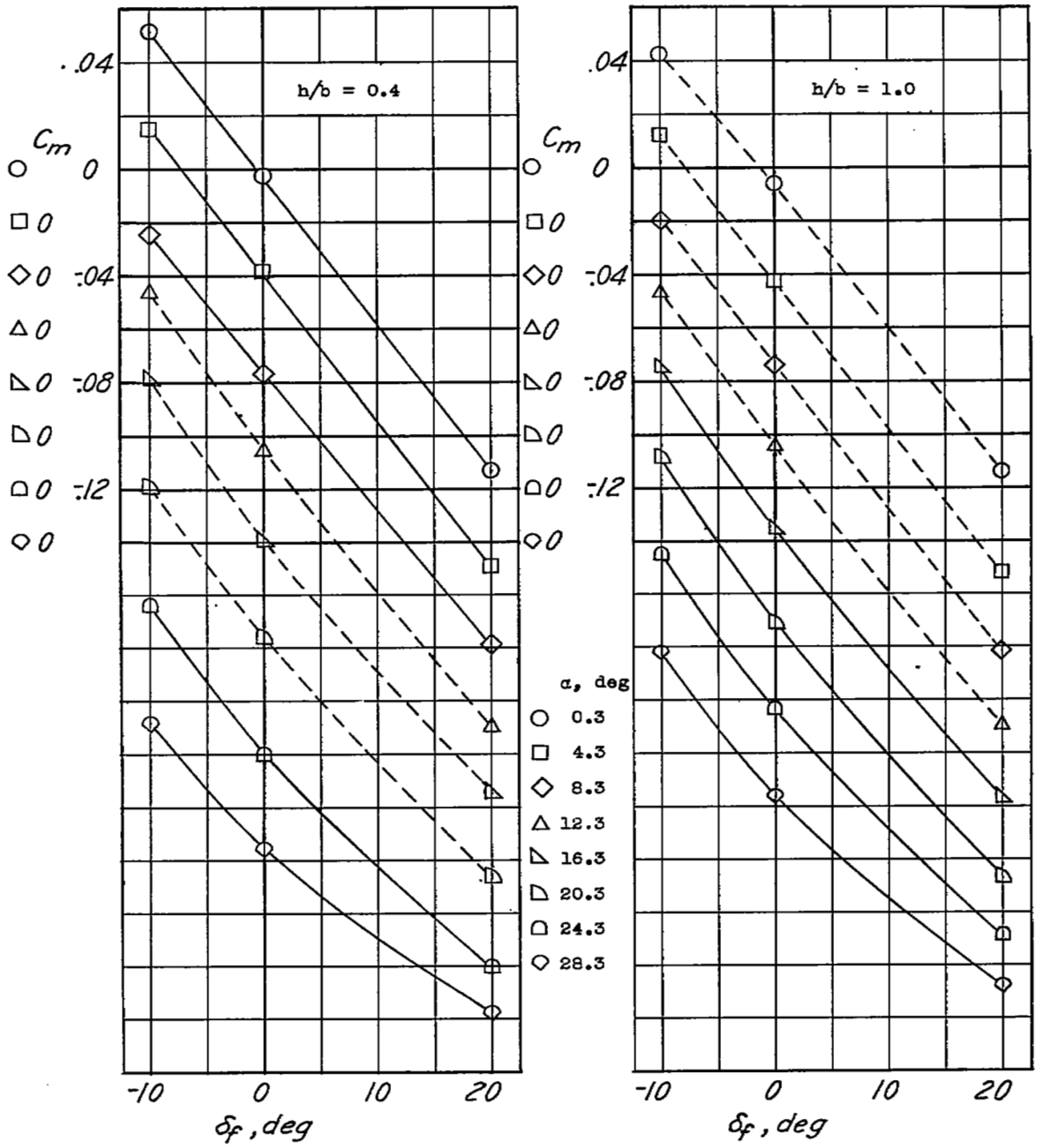

Figure 14.- Variation of pitching-moment coefficient with flap deflection at two ground heights. $\delta_a = 0^\circ$.

[redacted]

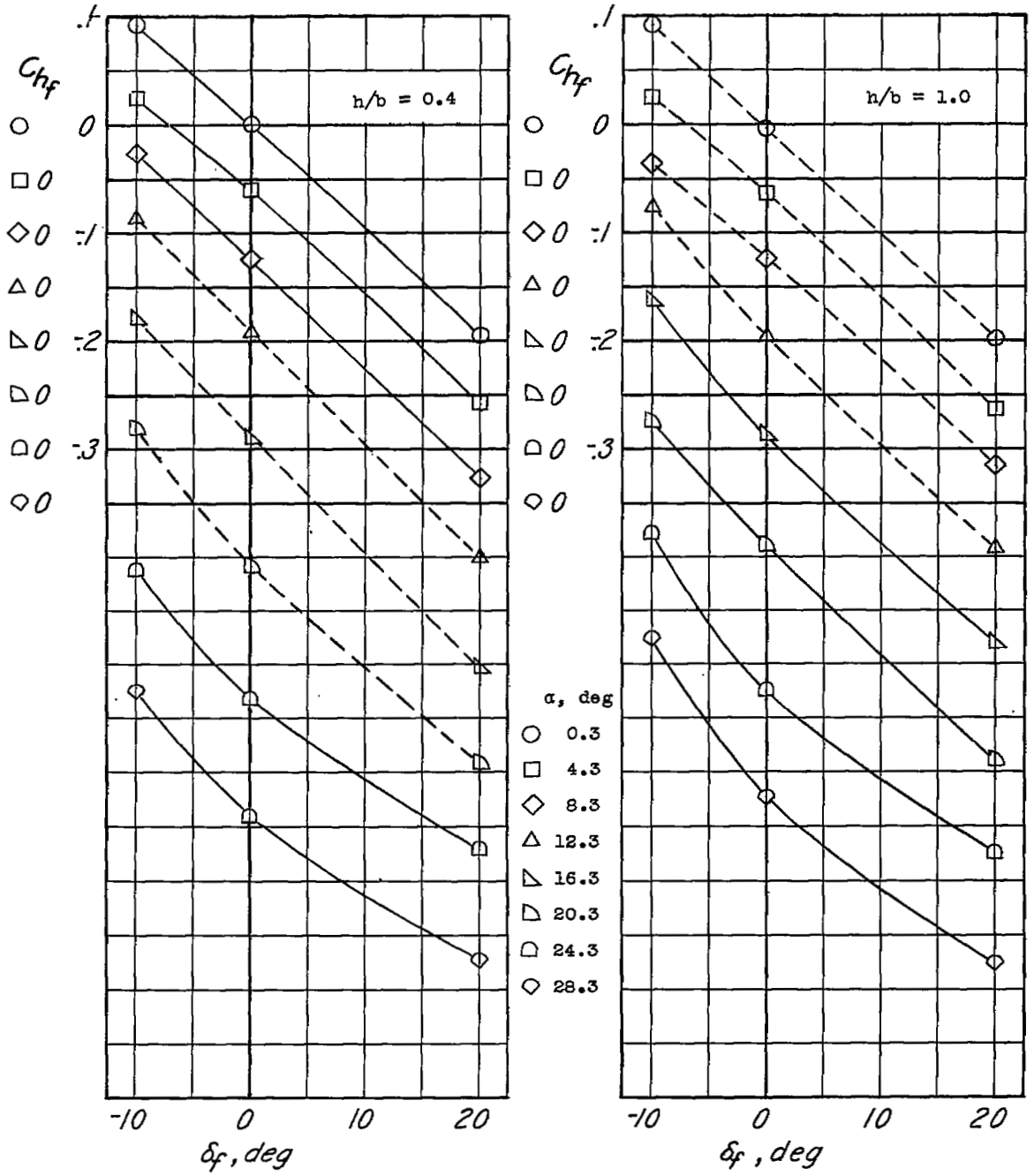

Figure 15.- Variation of hinge-moment coefficient with flap deflection at two ground heights. $\delta_a = 0^\circ$.

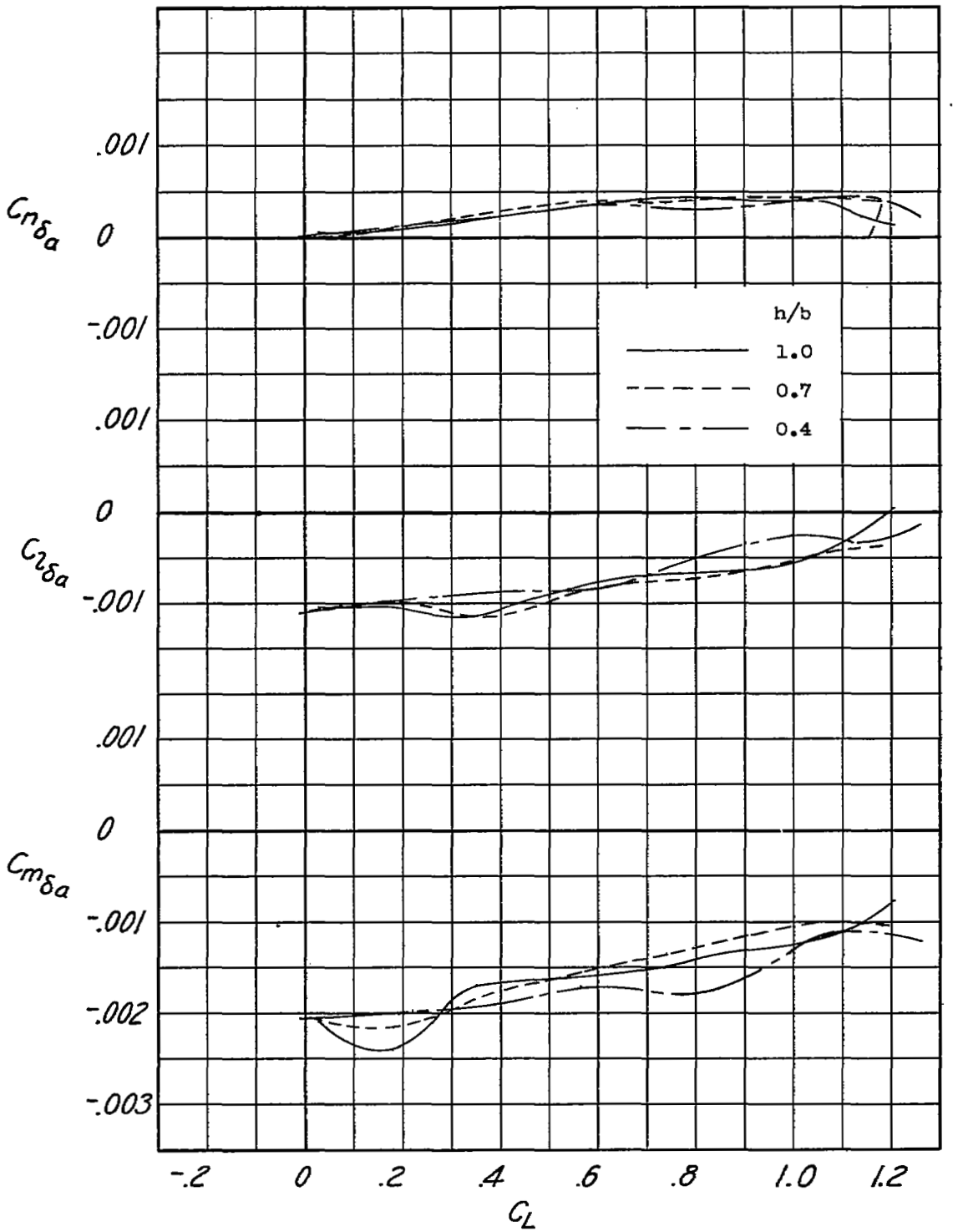

Figure 16.- Variation of aileron-control-effectiveness parameters with lift coefficient at three ground heights. $\delta_f = 0^\circ$.

[redacted]

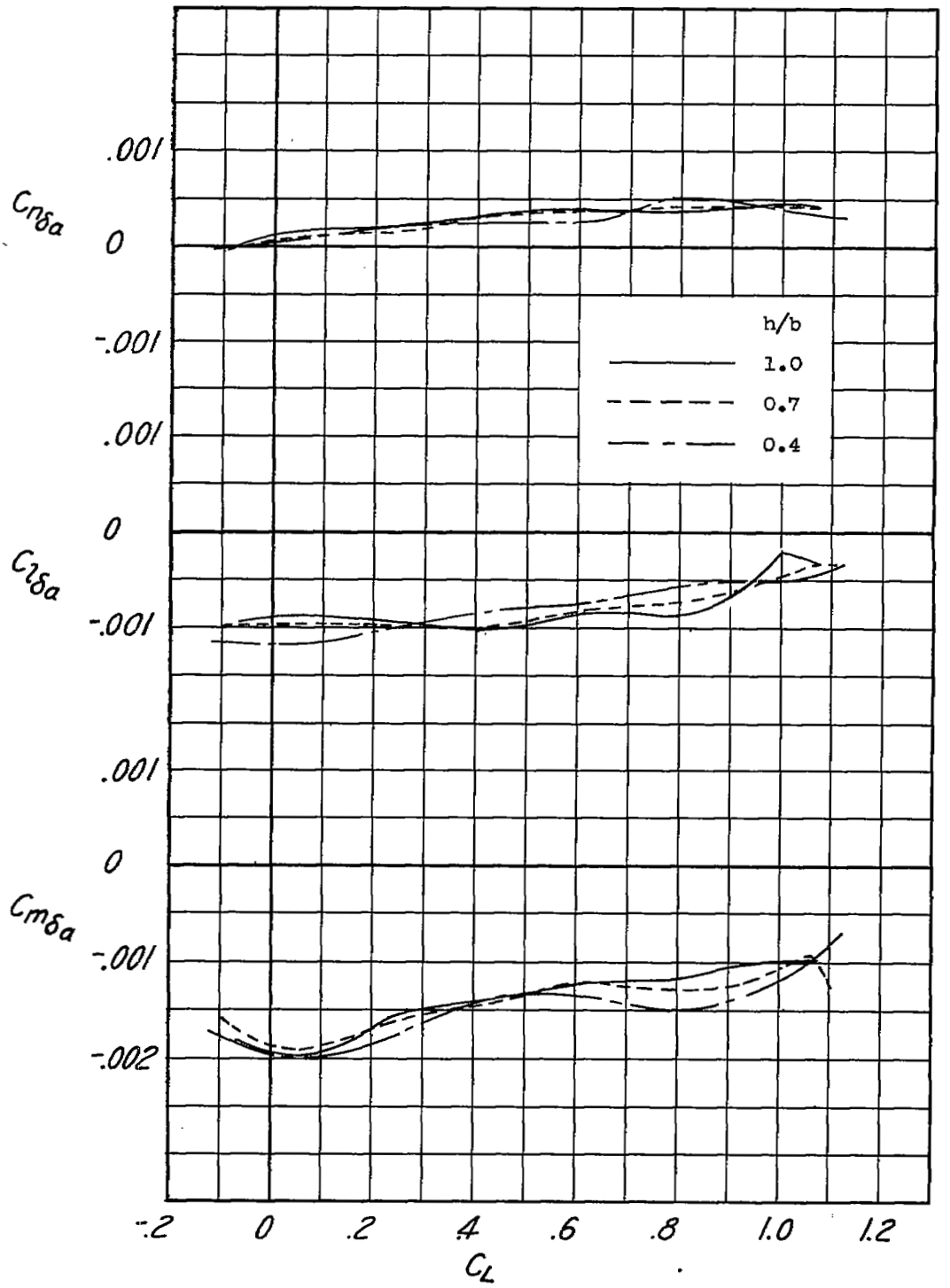

Figure 17.- Variation of aileron-control-effectiveness parameters with lift coefficient at three ground heights. $\delta_f = -10^\circ$.

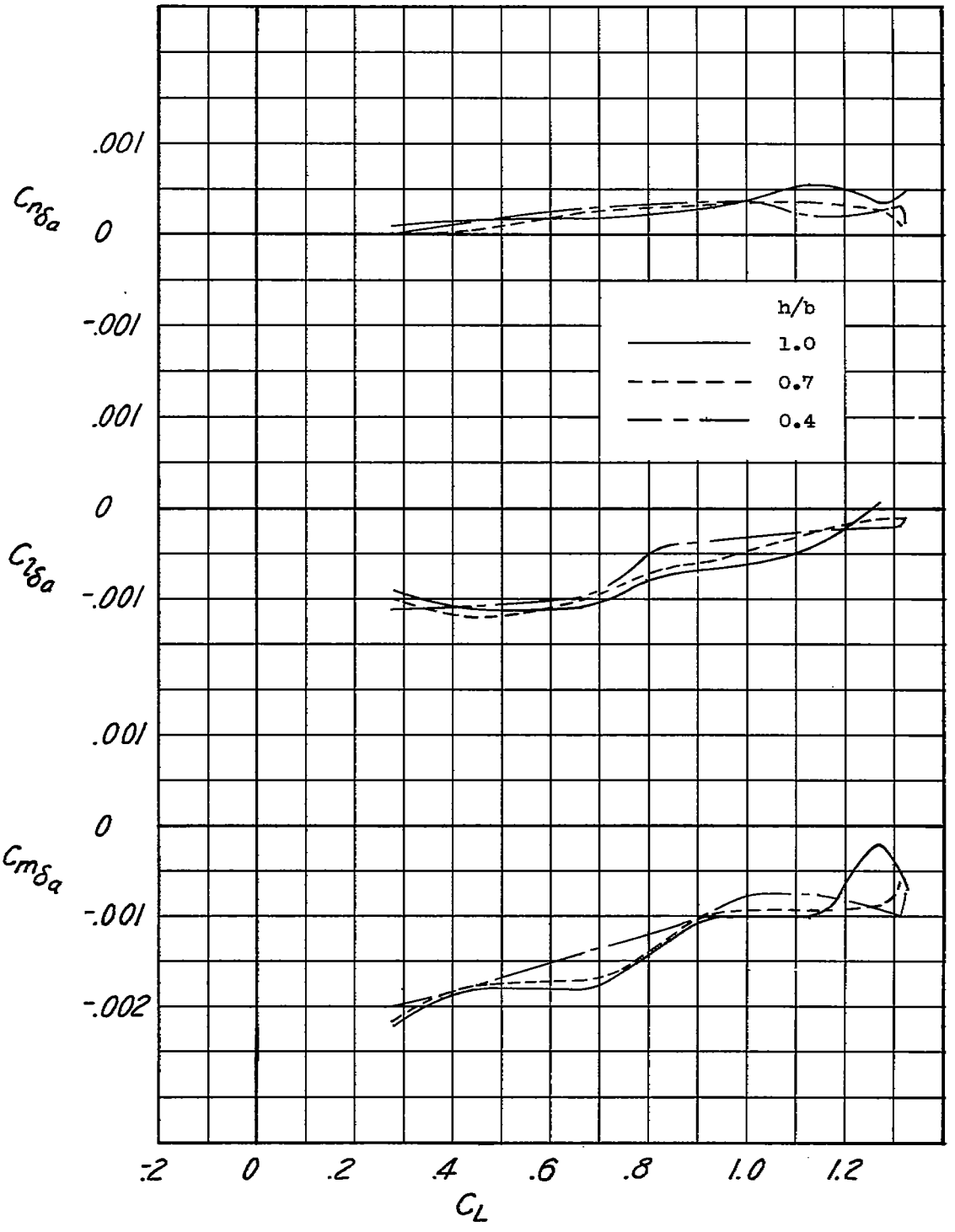

Figure 18.- Variation of aileron-control-effectiveness parameters with lift coefficient at three ground heights. $\delta_f = 20^\circ$.

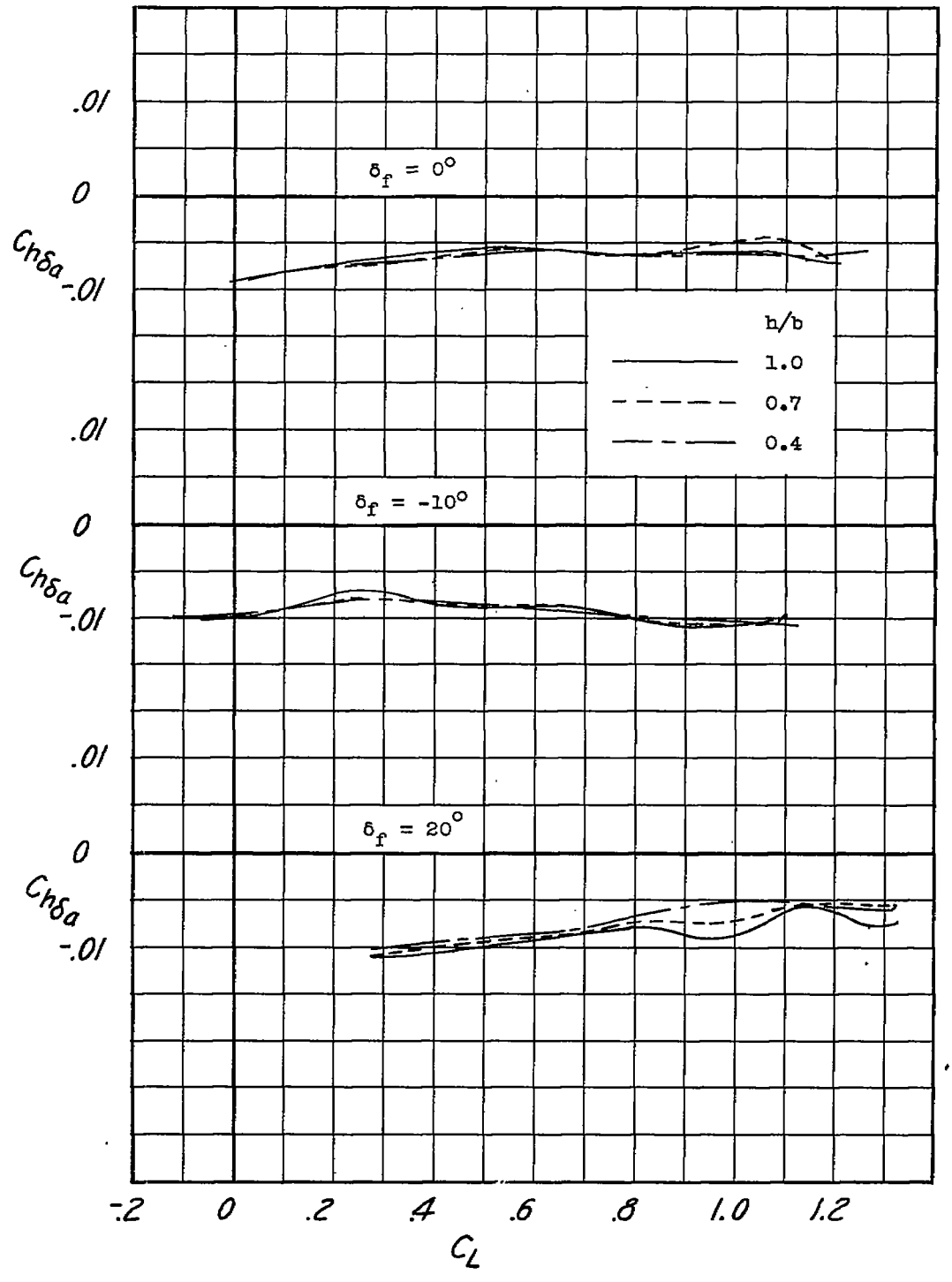

Figure 19.- Variation of aileron hinge-moment parameters with lift coefficient at three ground heights and three flap deflections.

[redacted]

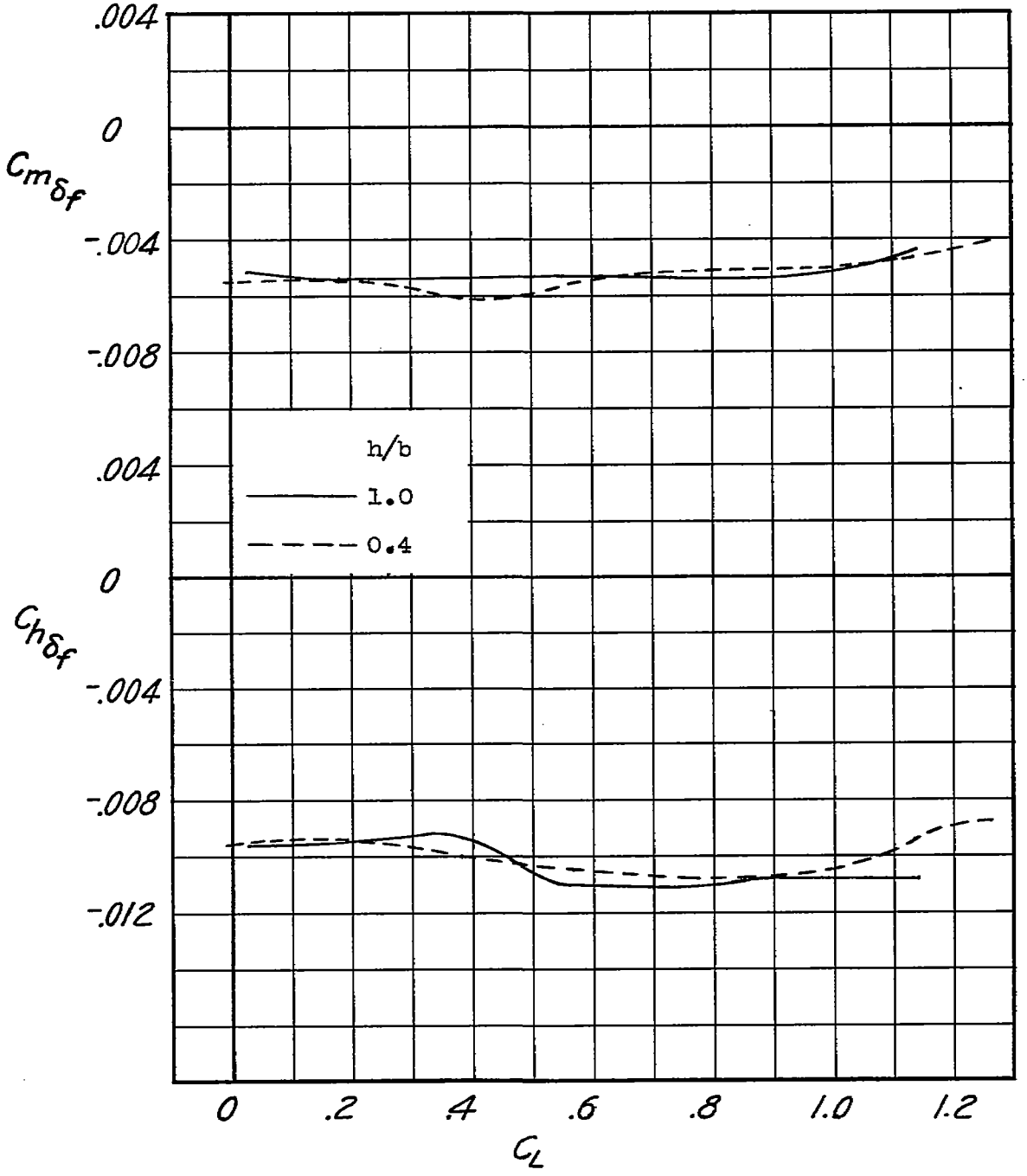

Figure 20.- Variation of flap control and hinge-moment parameters with lift coefficient at two ground heights. $\delta_a = 0^\circ$.

[redacted]

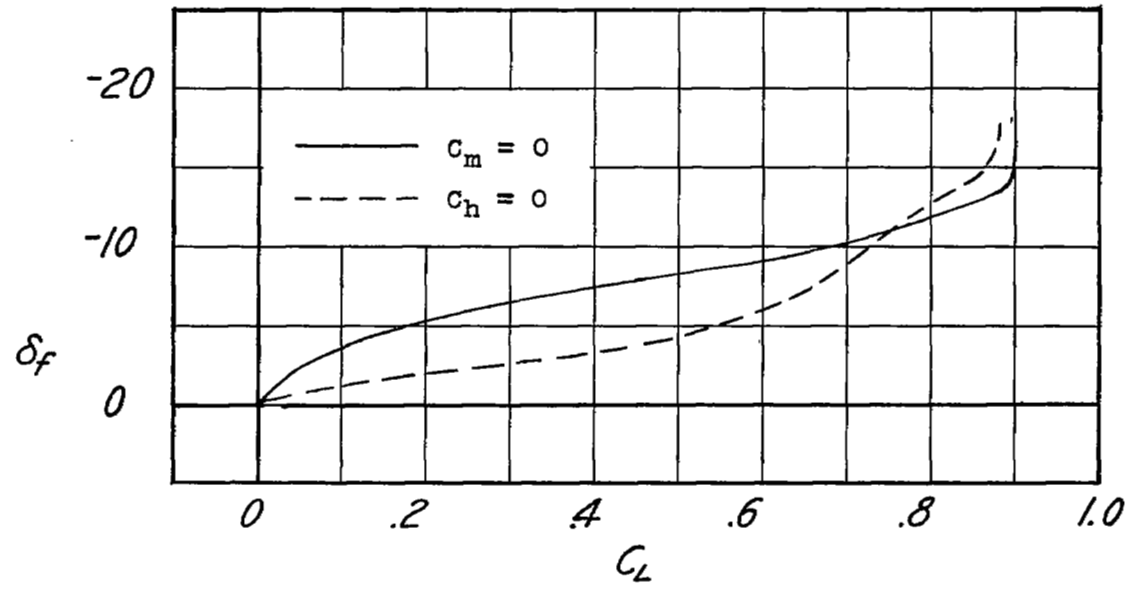

(a) h/b = 1.0.

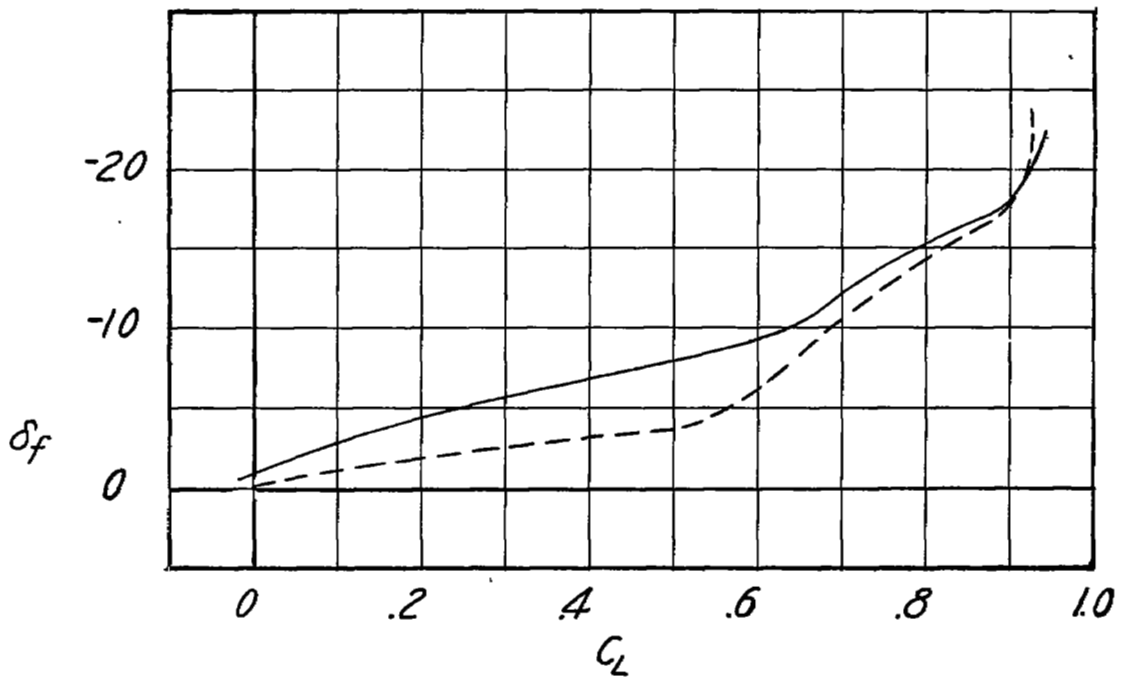

(b) h/b = 0.4.

Figure 21.- Variation of flap deflection required for trim and floating angle of the flap with lift coefficient at two ground heights. $\delta_a = 0^\circ$.

NACA-Langley - 9-24-54 - 350